

XYZ Meson Spectroscopy

Stephen Lars Olsen^{*†}

Center for Underground Physics, Institute for Basic Science

Daejeon 305-811, Republic of Korea

E-mail: solsensnu@gmail.com

Many candidate multiquark mesons, *i.e.*, mesons with substructures that are more complex than the quark-antiquark prescription that is in the textbooks, have recently been observed. Many of the most recently observed candidate states are electrically charged and have the same spin and parity, namely $J^P = 1^+$. In this talk I give an overview of the current experimental situation and identify patterns among the recently discovered $J^P = 1^+$ states, compare these patterns with expectations from proposed theoretical models, and the existence of additional, related states that might be accessible at current and future experiments. In addition, models that attribute the observed states to kinematically induced cusps are discussed.

53rd International Winter Meeting on Nuclear Physics

26-30 January 2015

Bormio, Italy

^{*}Speaker.

[†]This work supported under Project Code IBS-R001-D1.

1. Introduction

The strongly interacting particles of the Standard Model are colored quarks and gluons. In contrast, the strongly interacting particles in nature are color-singlet (*i.e.*, white) mesons and baryons. In the theory, quarks and gluons are related to mesons and baryons by the long-distance regime of Quantum Chromodynamics (QCD), which remains the least understood aspect of the theory. Since first-principle lattice-QCD (LQCD) calculations are still not practical for most long-distance phenomena,¹ a number of models motivated by the color structure of QCD have been proposed. However, so far at least, predictions of these QCD-motivated models that pertain to the spectrum of hadrons have not had great success.

For example, it is well known that combining a $q = u, d, s$ light-quark triplet with a $\bar{q} = \bar{u}, \bar{d}, \bar{s}$ light-antiquark antitriplet gives the familiar meson octet of flavor- $SU(3)$. Using similar considerations based on QCD, two quark triplets can be combined to form a “diquark” antitriplet of antisymmetric qq states and a sextet of symmetric qq states as illustrated in Fig. 1a. In QCD, these diquarks have color: combining a red triplet with a blue triplet – as shown in the figure – produces a magenta (anti-green) diquark and, for the antisymmetric triplet configuration, the color force between the two quarks is expected to be attractive. Likewise, green-red and blue-green diquarks form yellow (anti-blue) and cyan (anti-red) antitriplets as shown in Fig. 1b.

Since these diquarks are not color-singlets, they cannot exist as free particles but, on the other hand, the anticolored diquark antitriplets should be able to combine with other colored objects in a manner similar to antiquark antitriplets, thereby forming multi-quark color-singlet states with a more complex substructure than the $q\bar{q}$ mesons and qqq baryons of the original quark model [2]. These so-called “exotic” states include pentaquark baryons, six-quark H -dibaryons, and tetraquark mesons, as illustrated in Fig. 1c. Other proposed exotic states are: *glueballs*, which are mesons made only from gluons; *hybrids* formed from a q, \bar{q} and a gluon; and *molecules*, which are deuteron-like bound states of color-singlet “normal” hadrons [3]. These are illustrated in Fig. 1d. Glueball and hybrid mesons are motivated by QCD; molecules are a generalization of classical nuclear physics to systems of subatomic particles.

2. Searches for Exotic Hadrons in Light-Quark Systems

Of the proposed “multi-quark” states, pentaquarks have probably attracted the most theoretical and experimental attention [4]. However, in spite of some dramatic false alarms [5], there is no strong evidence for the existence of pentaquarks in nature [6, 7]. The absence of pentaquarks led Wilczek to remark “*The story of the pentaquark shows how poorly we understand QCD*” [8]. As for the six-quark H -dibaryon state, its strong theoretical motivation [9] has inspired numerous experimental searches [10]. However, to date, no evidence for it has been seen. The lack of any sign of the H -dibaryon (among other things) led Jaffe to observe that “*The absence of exotics is one of the most obvious features of QCD*” [11].

The experimental case for baryonium, a nucleon-antinucleon bound state [12], is more promising. While searches for narrow gamma-ray lines produced inclusively by at-rest $p\bar{p}$ annihilations found no signals [13], a strong threshold enhancement in the $p\bar{p}$ mass spectrum for radiative

¹This might not be the case for very much longer. Recent progress in this area has been impressive [1].

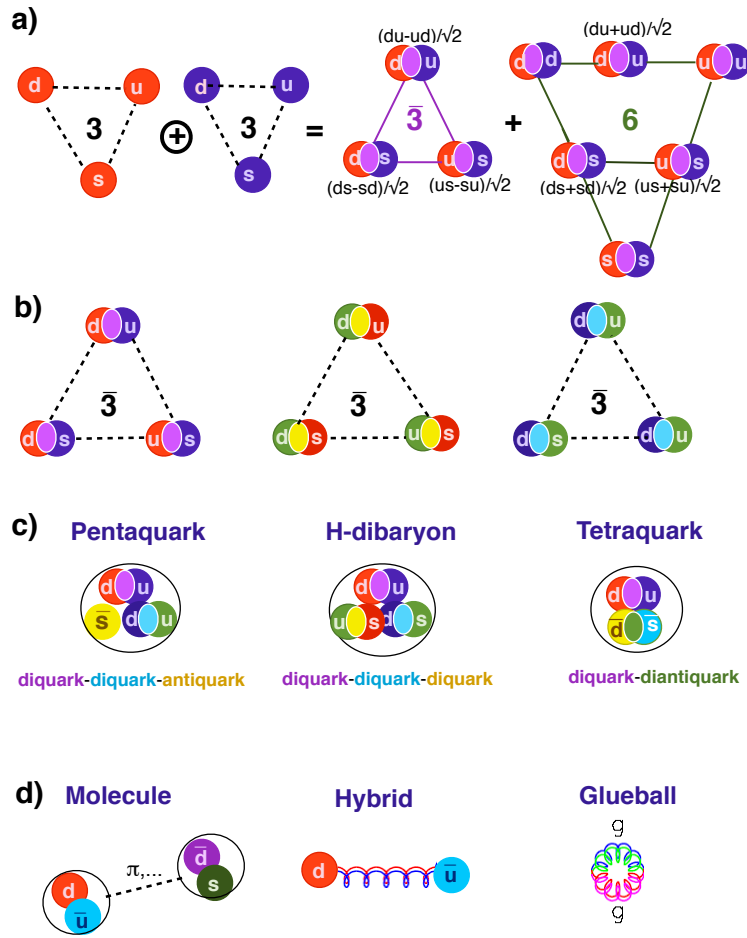


Figure 1: a) Combining a red and blue quark triplet produces a magenta (antigreen) antitriplet and sextet. b) The three anticolored diquark antitriplets. c) Some of the multiquark, color-singlet states that can be formed from quarks, antiquarks, diquarks and diantiquarks. d) Other possible multiquark/gluon systems.

$J/\psi \rightarrow \gamma p \bar{p}$ decays, reported by the BESII collaboration in 2003 [14], may be the tail of an S -wave $p \bar{p}$ bound state. Similar structures are not seen in the $p \bar{p}$ systems produced in $J/\psi \rightarrow \omega p \bar{p}$ [15] or $\Upsilon(1S) \rightarrow \gamma p \bar{p}$ [16] decays, which suggests that the observed structure cannot be entirely attributable to final-state-interactions between the p and \bar{p} . Different theoretical attempts to understand this threshold structure give contradictory results. An analysis based on an $N\bar{N}$ interaction derived in the framework of chiral effective field theory [17] finds an isovector $N\bar{N}$ bound state 37 MeV below the $2m_p$ mass threshold [18]. In contrast, an analysis based on the Paris $N\bar{N}$ potential [19], attributes the threshold enhancement to the tail of an isospin singlet $^1S_0 N\bar{N}$ state with a mass that is 4.8 MeV below threshold [20].² This latter analysis also predicts a nearby triplet P -wave state.

Two candidates for exotic light-quark mesons, the $J^{PC} = 1^{-+} \pi_1(1600)$ [21], and a new re-

²In this report the convention $c = 1$ is used.

sult from COMPASS, the $1^{++} a_1(1420)$ [22], were discussed at this meeting by Ketzer [23]. The $\pi_1(1600)$ has explicitly exotic³ quantum numbers. However, because strong rescattering effects are expected to provide significant backgrounds with 1^{-+} quantum numbers, questions have been raised about the interpretation of the $\pi_1(1600)$ signals as a true resonance [24]. COMPASS sees strong $\pi_1(1600) \rightarrow \eta' \pi$ signals in $\pi^- p \rightarrow \pi^- \eta' p$ reactions with large four-momentum transfer to the proton, where rescattering effects are expected to be small. However, a full analysis of these new data is not yet available. The $a_1(1420)$ shows up as a peak in the $1^{++} f_0(980)\pi$ P -wave produced in $\pi^- p \rightarrow f_0(980)\pi^- p$ reactions. Although it does not have exotic quantum numbers, it is unusual in that its mass (1412~1422 MeV) is too low and width (130~150 MeV) too narrow to be considered as a reasonable candidate for a radial excitation of the well established 1^{++} ground state meson, the $a_1(1260)$. Ketzer cautioned that the $a_1(1420)$ mass peak is just above the $K^*(890)\bar{K}$ mass threshold ($m_{K^*(890)} + m_K \simeq 1390$ MeV), and the rescattering process $a_1(1260) \rightarrow K^*(890)\bar{K} \rightarrow f_0(980)\pi$ can produce a cusp-like peak in the $f_0(980)\pi$ invariant mass distribution that is unrelated to any resonance and dangerously close to 1420 MeV. Moreover, the finite width and Breit-Wigner phase of the $K^*(890)$ resonance can produce a phase motion that might mimic that of a real resonance. I discuss rescattering induced, near-threshold cusp effects below, albeit in a somewhat different context.

3. Charmonium and the XYZ Mesons

Charmonium mesons are states that can be formed from a charmed (c) and anticharmed (\bar{c}) quark pair. Since the charmed quark is relatively massive ($m_c \simeq 1.3$ GeV), the constituent velocities in charmonium mesons are relatively small ($v^2/c^2 \simeq 0.2$) and relativistic effects can be treated as perturbative corrections to ordinary Quantum Mechanical calculations [25, 26]. The mass spectrum of experimentally established charmonium states is indicated by the yellow rectangles in Fig. 2; all of the expected states with mass below the $2m_D$ open-charmed threshold have been assigned. The gray rectangles indicate remaining unassigned levels that are below 4.5 GeV.

The large c -quark mass is expected to suppress the production of $c\bar{c}$ pairs via quark→hadron fragmentation processes at $E_{\text{cm}} \leq \sim 10$ GeV to an insignificant level [27]. Thus, if a newly observed meson state decays into final states that contain a c - and \bar{c} -quark pair, those quarks must be present in the initial-state particle. If the initial-state particle's constituents are only the c - and the \bar{c} -quarks, then the particle is necessarily a charmonium meson and must occupy one of the unassigned levels in the charmonium spectrum, (*i.e.*, one of the gray rectangles in Fig. 2). Similar remarks apply to meson states that are seen to decay to final states containing a b and \bar{b} quark pair and the bottomonium ($b\bar{b}$) meson spectrum.

3.1 The XYZ mesons

The XYZ mesons are an assortment of recently discovered resonance-like structures in hadronic final states that contain either a c and \bar{c} , or a b and \bar{b} quark pair, with properties that do not match to expectations for any of the currently unassigned $c\bar{c}$ charmonium or $b\bar{b}$ bottomonium states. In Fig. 2, the charmoniumlike XYZ mesons are indicated as red and purple rectangles aligned

³Quantum numbers that cannot be accessed by a $q\bar{q}$ system, *e.g.* 0^{--} , 0^{+-} , 1^{-+} , 2^{+-} etc., are called “exotic.”

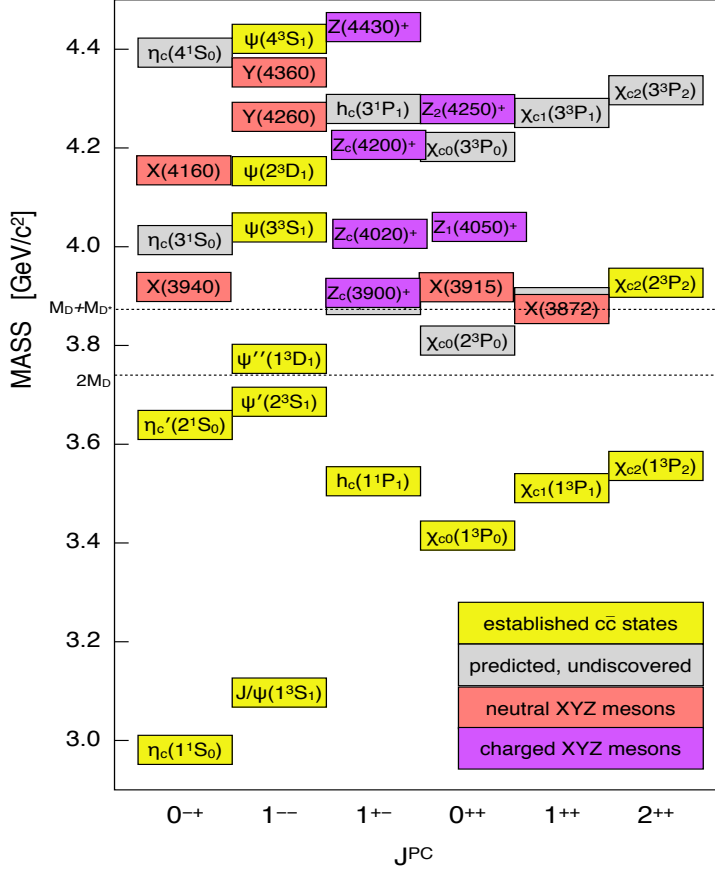


Figure 2: The spectrum of charmonium and charmoniumlike mesons.

according to my best guess at their J^{PC} quantum numbers. A reasonably up-to-date list of the XYZ candidate states, together with some of their essential properties, is provided in Table 1 and some recent reviews can be found in Refs. [28, 29, 30, 31].⁴ The designation of these states as X, Y, or Z was initially haphazard, but now has settled into a pattern in which researchers engaged in this field (but not the Particle Data Group (PDG) [21]) designate $J^{PC} = 1^{--}$ neutral states as Y, those with isospin=1 as Z, and all of the rest as X. However, a few exceptions to this pattern persist.

3.2 A whirlwind tour

Moving from left to right in Fig. 2, I review reasons that the XYZ states are poor matches for any of the unassigned charmonium states. (Experimental references are given in Table 1.)

⁴In Table 1 and the rest of this report, the inclusion of charge conjugate states is always implied.

Table 1: The XYZ mesons. Masses M and widths Γ are weighted averages with uncertainties added in quadrature. Only $\pi^+\pi^-J/\psi$ decays are used in the $X(3872)$ mass average. Ellipses (...) indicate inclusive reactions. Question marks indicate best guesses or no J^{PC} information. For charged states, C refers to the neutral isospin partner.

State	M (MeV)	Γ (MeV)	J^{PC}	Process (decay mode)	References
$X(3872)$	3871.68 ± 0.17	< 1.2	1^{++}	$B \rightarrow K + (J/\psi \pi^+ \pi^-)$	[32, 33, 34, 35]
				$p\bar{p} \rightarrow (J/\psi \pi^+ \pi^-) + \dots$	[36, 37, 38, 39, 40]
				$B \rightarrow K + (J/\psi \pi^+ \pi^- \pi^0)$	[41, 42]
				$B \rightarrow K + (D^0 \bar{D}^0 \pi^0)$	[43, 44]
				$B \rightarrow K + (J/\psi \gamma)$	[45, 46, 47]
				$B \rightarrow K + (\psi' \gamma)$	[45, 46, 47]
				$pp \rightarrow (J/\psi \pi^+ \pi^-) + \dots$	[48, 49]
$X(3915)$	3917.4 ± 2.7	28_{-9}^{+10}	0^{++}	$B \rightarrow K + (J/\psi \omega)$	[50, 42]
$X(3940)$	3942_{-8}^{+9}	37_{-17}^{+27}	$0(?)^{-(?)^+}$	$e^+e^- \rightarrow e^+e^- + (J/\psi \omega)$	[51, 52]
				$e^+e^- \rightarrow J/\psi + (D^* \bar{D})$	[53]
$G(3900)$	3943 ± 21	52 ± 11	1^{--}	$e^+e^- \rightarrow J/\psi + (\dots)$	[54]
				$e^+e^- \rightarrow \gamma + (D \bar{D})$	[55, 56]
$Y(4008)$	4008_{-49}^{+121}	226 ± 97	1^{--}	$e^+e^- \rightarrow \gamma + (J/\psi \pi^+ \pi^-)$	[57]
$Y(4140)$	4144 ± 3	17 ± 9	$?^{2+}$	$B \rightarrow K + (J/\psi \phi)$	[58, 59, 60]
$X(4160)$	4156_{-25}^{+29}	139_{-65}^{+113}	$0(?)^{-(?)^+}$	$e^+e^- \rightarrow J/\psi + (D^* \bar{D})$	[53]
$Y(4260)$	4263_{-9}^{+8}	95 ± 14	1^{--}	$e^+e^- \rightarrow \gamma + (J/\psi \pi^+ \pi^-)$	[61, 62, 63, 57]
				$e^+e^- \rightarrow (J/\psi \pi^+ \pi^-)$	[64]
				$e^+e^- \rightarrow (J/\psi \pi^0 \pi^0)$	[64]
$Y(4360)$	4361 ± 13	74 ± 18	1^{--}	$e^+e^- \rightarrow \gamma + (\psi' \pi^+ \pi^-)$	[65, 66]
$X(4630)$	4634_{-11}^{+9}	92_{-32}^{+41}	1^{--}	$e^+e^- \rightarrow \gamma (\Lambda_c^+ \Lambda_c^-)$	[67]
$Y(4660)$	4664 ± 12	48 ± 15	1^{--}	$e^+e^- \rightarrow \gamma + (\psi' \pi^+ \pi^-)$	[66]
$Z_c^+(3900)$	3890 ± 3	33 ± 10	1^{+-}	$Y(4260) \rightarrow \pi^- + (J/\psi \pi^+)$	[68, 69]
				$Y(4260) \rightarrow \pi^- + (D \bar{D}^*)^+$	[70]
$Z_c^+(4020)$	4024 ± 2	10 ± 3	$1(?)^{+(?)^-}$	$Y(4260) \rightarrow \pi^- + (h_c \pi^+)$	[71]
				$Y(4260) \rightarrow \pi^- + (D^* \bar{D}^*)^+$	[72]
$Z_c^0(4020)$	4024 ± 4	10 ± 3	$1(?)^{+(?)^-}$	$Y(4260) \rightarrow \pi^0 + (h_c \pi^0)$	[73]
$Z_1^+(4050)$	4051_{-43}^{+24}	82_{-55}^{+51}	$?^{2+}$	$B \rightarrow K + (\chi_{c1} \pi^+)$	[74, 75]
$Z^+(4200)$	4196_{-32}^{+35}	370_{-149}^{+99}	1^{+-}	$B \rightarrow K + (J/\psi \pi^+)$	[76]
$Z_2^+(4250)$	4248_{-45}^{+185}	177_{-72}^{+321}	$?^{2+}$	$B \rightarrow K + (\chi_{c1} \pi^+)$	[74, 75]
$Z^+(4430)$	4477 ± 20	181 ± 31	1^{+-}	$B \rightarrow K + (\psi' \pi^+)$	[77, 78, 79, 80]
				$B \rightarrow K + (J\psi \pi^+)$	[76]
$Y_b(10890)$	10888.4 ± 3.0	$30.7_{-7.7}^{+8.9}$	1^{--}	$e^+e^- \rightarrow (\Upsilon(nS) \pi^+ \pi^-)$	[81]
$Z_b^+(10610)$	10607.2 ± 2.0	18.4 ± 2.4	1^{+-}	$\Upsilon(5S) \rightarrow \pi^- + (\Upsilon(1, 2, 3S) \pi^+)$	[82, 83]
				$\Upsilon(5S) \rightarrow \pi^- + (h_b(1, 2P) \pi^+)$	[82]
				$\Upsilon(5S) \rightarrow \pi^- + (B \bar{B}^*)^+$	[84]
$Z_b^0(10610)$	10609 ± 6		1^{+-}	$\Upsilon(5S) \rightarrow \pi^0 + (\Upsilon(1, 2, 3S) \pi^0)$	[85]
$Z_b^+(10650)$	10652.2 ± 1.5	11.5 ± 2.2	1^{+-}	$\Upsilon(5S) \rightarrow \pi^- + (\Upsilon(1, 2, 3S) \pi^+)$	[82]
				$\Upsilon(5S) \rightarrow \pi^- + (h_b(1, 2P) \pi^+)$	[82]
				$\Upsilon(5S) \rightarrow \pi^- + (B^* \bar{B}^*)^+$	[84]

The X(3940) and X(4160) are seen in the invariant mass distributions of the $D\bar{D}^*$ and $D^*\bar{D}^*$ systems that recoil from the J/ψ in $e^+e^- \rightarrow J/\psi D^{(*)}\bar{D}^*$ reactions at $E_{\text{cm}} \simeq 10.6$ GeV, respectively. The only known charmonium states that are seen recoiling from a J/ψ in these processes, the η_c , χ_{c0} and $\eta_c(2S)$, all have spin=0 [86, 87]. This, plus the fact that neither the X(3940) nor the X(4160) is seen to decay to $D\bar{D}$ [53], provides circumstantial evidence for $J^{PC} = 0^{-+}$. The unassigned 0^{-+} charmonium states are the $\eta_c(3S)$ and $\eta_c(4S)$, which are expected to have masses around 4010 and 4390 MeV, respectively [26]. The $X(3940) = \eta_c(3S)$ and $X(4160) = \eta_c(4S)$ assignments would imply anomalously large $\psi(nS)$ - $\eta_c(nS)$ mass splittings for $n = 3$ of ~ 120 MeV, and $n = 4$ of ~ 260 MeV, which are both huge compared to theoretical expectations of ~ 30 and ~ 25 MeV, respectively [26, 88].

The Y(4260) and Y(4360) were first seen in the $\pi^+\pi^-J/\psi$ and $\pi^+\pi^-\psi'$ mass distributions, respectively, in the initial-state-radiation (ISR) processes $e^+e^- \rightarrow \gamma_{\text{ISR}}\pi^+\pi^-J/\psi(\psi')$. This production mechanism ensures that J^{PC} quantum numbers for these state are 1^{--} . All of the 1^{--} charmonium states with masses below 4.5 GeV have already been established [89]; there are no available slots for either the Y(4260) or the Y(4360).

The $Z_c(3900)$, $Z_c(4020)$, $Z_c(4200)$, $Z(4430)$, $Z_1(4050)$ and $Z_2(4250)$ are seen in π^+J/ψ , π^+h_c , $\pi^+\psi'$ or $\pi^+\chi_{c1}$ invariant mass spectra and, thus, have a non-zero electric charge. Charmonium states, by definition, are $c\bar{c}$ states with zero charge (and isospin). The first four have $J^{PC} = 1^{++}$ quantum numbers,⁵ where here, and in the rest of this report, C refers to the C -parity of the neutral member of the isospin triplet. Although the Z_1 and Z_2 necessarily have even C -parity, they could have any J^P value other than 0^- , which is forbidden by parity. The BESIII and Belle experimental signals for the charged Z states were discussed at this meeting by Gradl [90] and Lange [91].

The X(3915) is seen as $\omega J/\psi$ invariant mass peaks in $B \rightarrow K\omega J/\psi$ decays and in $\gamma\gamma \rightarrow \omega J/\psi$ two-photon fusion reactions. A BaBar study of the latter process concluded that $J^{PC} = 0^{++}$ [52]. BaBar (and the PDG) identify this state as the $\chi_{c0}(2P)$, the first radial excitation of the χ_{c0} charmonium state. This assignment has some serious problems: the mass is too high; the total width is too narrow; decays to $D\bar{D}$ final states, which should be the dominant decay mode for the $\chi_{c0}(2P)$, are not seen; and the production rates in B decays and $\gamma\gamma$ fusion are incompatible with a $\chi_{c0}(2P)$ assignment [92, 93].

The X(3872) was the first XYZ meson to be discovered and is the most well studied. I discuss its properties in some detail in the following section.

4. The X(3872)

The X(3872) was first seen by Belle as a narrow peak in the $\pi^+\pi^-J/\psi$ invariant mass distribution in exclusive $B \rightarrow K\pi^+\pi^-J/\psi$ decays [32] (see Fig 3a). It is a well established state that has been seen by (at least) six other experiments [34, 36, 40, 48, 49, 94].

⁵This includes an ‘‘informed guess’’ for the J^P of the $Z_c(4020)$ that is discussed below in Section 5.2.2.

4.1 Properties of the X(3872)

The most striking feature of the X(3872) is the virtual indistinguishability between its measured mass, $M_{X(3872)} = 3871.69 \pm 0.17$ MeV [21], and the sum of the D^0 and D^{*0} masses, $m_{D^0} + m_{D^{*0}} = 3871.69 \pm 0.09$ MeV [95]. Also striking is its narrow total width, $\Gamma_{X(3872)} < 1.2$ MeV (90% CL) [33]. The $X(3872) \rightarrow \gamma J/\psi$ decay mode has been seen by BaBar [45], Belle [46], and LHCb [47] with a branching fraction that is 0.24 ± 0.05 that for $X(3872) \rightarrow \pi^+ \pi^- J/\psi$. BaBar and LHCb group report signals for $X(3872) \rightarrow \gamma \psi'$ with a branching fraction that is 2.7 ± 0.6 times that for $X(3872) \rightarrow \gamma J/\psi$. The $M(\pi^+ \pi^-)$ distribution for $X(3872) \rightarrow \pi^+ \pi^- J/\psi$, shown in Fig. 3b, is consistent with expectations for $\rho \rightarrow \pi^+ \pi^-$ decays [33, 37]. The $X(3872) \rightarrow \omega J/\psi$ decay mode has been seen with a branching fraction that is similar to that for $\rho J/\psi$ [41, 42] even though the decay phase space only covers a small fraction of the ω resonance's low mass tail. These observations clearly establish that the C-parity of the X(3872) is $C = +1$ and that isospin is strongly violated in its decays. A CDF study of $X(3872) \rightarrow \pi^+ \pi^- J/\psi$ decays limited the J^{PC} quantum numbers to be either 1^{++} or 2^{-+} [38]; a subsequent LHCb comparison of these two possibilities using $X(3872) \rightarrow \pi^+ \pi^- J/\psi$ events produced via B meson decay unambiguously favored $J^{PC} = 1^{++}$ [35]. The X(3872) has a significant coupling to $D^0 \bar{D}^{*0}$ that is seen by both Belle [43] and Babar [44] as a pronounced threshold enhancement in the $M(D^0 \bar{D}^{*0})$ distribution in $B \rightarrow KD^0 \bar{D}^{*0}$ decays; the Belle results are shown in Fig. 3c. The X(3872) branching fraction to $D^0 \bar{D}^{*0}$ is 9.9 ± 3.2 times larger than that for $X(3872) \rightarrow \pi^+ \pi^- J/\psi$.

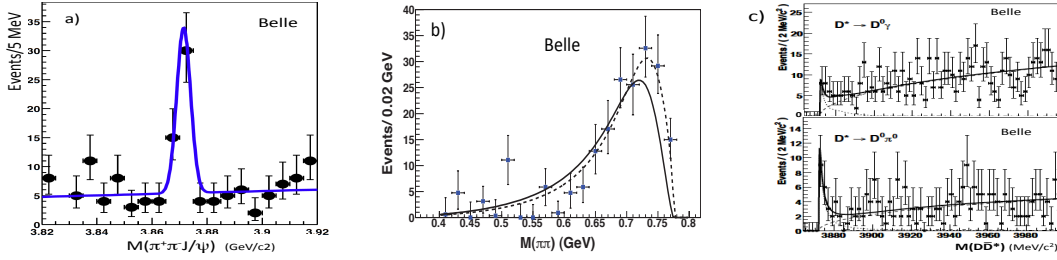


Figure 3: a) The $M(\pi^+ \pi^- J/\psi)$ distribution for $B \rightarrow K \pi^+ \pi^- J/\psi$ events from Belle's original X(3872) paper [32]. b) The $M(\pi^+ \pi^-)$ distribution for $X(3872) \rightarrow \pi^+ \pi^- J/\psi$ events from Belle [33]. The curves shows results of fits to a $\rho \rightarrow \pi^+ \pi^-$ line shape including ρ - ω interference. The dashed (solid) curve is for even (odd) X(3872) parity. c) $M(D^0 \bar{D}^{*0})$ distributions for $B \rightarrow KD^0 \bar{D}^{*0}$ decays from Belle [43]. The upper plot is for $\bar{D}^{*0} \rightarrow \bar{D}^0 \gamma$ decays, the lower plot is for $\bar{D}^{*0} \rightarrow \bar{D}^0 \pi^0$ decays. The peaks near threshold are attributed to $X(3872) \rightarrow D^0 \bar{D}^{*0}$ decays.

4.2 Prompt X(3872) production in high energy $\bar{p}(p)$ -p collisions

The $X(3872) \rightarrow \pi^+ \pi^- J/\psi$ signals seen in 1.96 TeV $p\bar{p}$ [36] and 7 TeV pp [49]) collisions are $7 \sim 10\%$ those for $\psi' \rightarrow \pi^+ \pi^- J/\psi$. Figure 4 shows CDF results for the proper-time dependence of X(3872) production in inclusive $p\bar{p} \rightarrow \pi^+ \pi^- J/\psi + X$ annihilations at $E_{\text{cm}} = 1.96$ TeV [96]. They find that only a small fraction of the X(3872) signal, shown in magenta, has a displaced vertex distribution that is characteristic of the B meson lifetime; $(84 \pm 5)\%$ of the X(3872) signal, shown in red, is produced promptly. A similar study of the $\psi' \rightarrow \pi^+ \pi^- J/\psi$ signal found $(72 \pm 1)\%$ of the ψ' signal is produced promptly. Results from a D0 comparison of the properties of X(3872) and ψ' production at the same energy are shown Fig. 5b [40]. Here the open circles show the fractions of the X(3872) signal that have: transverse momentum $p_T > 10$ GeV/c; pseudorapidity in

the range $|y| < 1$; pion (muon) helicity angle in the region $\cos\theta_{\pi(\mu)} < 0.4$; and isolation < 1 , where isolation is the ratio of $X(3872)$ momentum to the summed momenta of all other charged tracks within $\Delta R = 0.5$ of the $X(3872)$ direction ($\Delta R \equiv \sqrt{(\Delta y)^2 + (\Delta\phi)^2}$). These fractions agree quite well with the corresponding quantities for ψ' production, which are shown in the figure as solid squares.

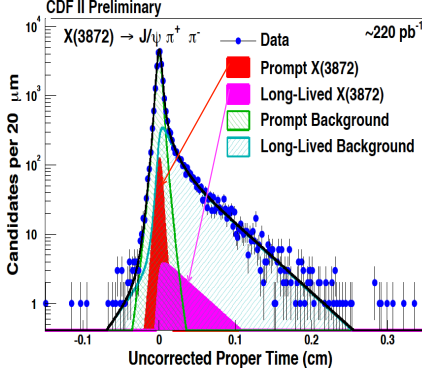


Figure 4: The uncorrected proper time distribution for $X(3872)$ production from CDF [96]

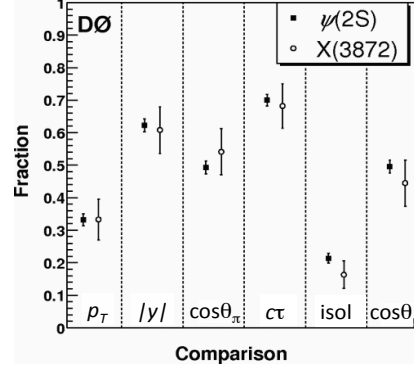


Figure 5: Comparison of $X(3872)$ and ψ' event-yield fractions for different measured quantities [40]. (See text for details.)

4.3 Charmonium assignment for the $X(3872)$?

The only unassigned conventional 1^{++} charmonium state that is expected to have a mass that is anywhere near 3872 MeV is the $\chi_{c1}(2P)$ (commonly called the χ'_{c1}), *i.e.*, the first radial excitation of the χ_{c1} . This assignment for the $X(3872)$ has some problems. The χ'_{c2} , the $J = 2$ spin-multiplet partner of the the χ'_{c1} , is well established with a measured mass of 3927.2 ± 2.6 MeV [21]. An $X(3872) = \chi'_{c1}$ assignment would imply a $\chi_{c2}(2P)$ - $\chi_{c1}(2P)$ mass splitting of $\Delta M_{2-1}(2P) = 55.5 \pm 2.6$ MeV, which is larger than the “ground-state” splitting $\Delta M_{2-1}(1P) = 45.5 \pm 0.1$ MeV. This behavior is contrary to potential model expectations, where these splittings are due to tensor and spin-orbit forces that decrease with increasing radius (and, therefore, radial quantum number) [25]. For states above open-charmed threshold, like the χ'_{c2} and, depending on its mass, the χ'_{c1} , potential model predictions are modified by couplings to on-mass-shell, open-charmed meson pair configurations. However, three different methods for computing these effects all find that they tend to suppress the χ'_{c2} mass while increasing that of the χ'_{c1} and, thereby, reducing (not increasing) this splitting to values that are below potential-model based expectations [88, 97, 98]. A second problem with the $X(3872) = \chi'_{c1}$ assignment is that the measured upper limit on its natural width ($\Gamma_{X(3872)} < 1.2$ MeV) is only slightly above the natural width of the “ground-state” χ_{c1} : $\Gamma_{\chi_{c1}} = 0.84 \pm 0.04$ MeV. Since the χ'_{c1} could access any of the χ_{c1} decay channels with significantly increased phase-space and have a number of additional decay channels, including decays to open-charmed mesons and hadronic & radiative transitions to $1P$ & $1S$ charmonium states, it is expected that its natural width would be substantially broader than that of the χ_{c1} . (All of the identified $X(3872)$ decay channels, which account for at least one third of its total decay width, are to final states that are kinematically inaccessible to the χ_{c1} , namely $D^0\bar{D}^0\pi^0(\gamma)$, $\rho J/\psi$, $\omega J/\psi$ and $\gamma\psi'$ [21].) A third problem with the $X(3872) = \chi'_{c1}$ assignment is that the decay $\chi'_{c1} \rightarrow \rho J/\psi$ vio-

lates isospin and is, therefore, expected to be strongly suppressed and unlikely to be a “discovery channel” for the χ'_{c1} .

4.4 If not charmonium, then what?

For these reasons, the $X(3872)$ is expected to have a more complex sub-structure than the simple $c\bar{c}$ configuration that is expected for the χ'_{c1} in charmonium potential models.

The near coincidence of its mass with the $D^0\bar{D}^{*0}$ mass threshold has led to considerable speculation that it is predominantly a molecule-like $X(3872) = (D^{*0}\bar{D}^0 + D^0\bar{D}^{*0})/\sqrt{2}$ configuration in which the (color-singlet) D and \bar{D}^* mesons are loosely bound by Yukawa-like nuclear forces [99] (see Fig. 1d), an idea that has been around for some time [3].

Other authors have interpreted the $X(3872)$ as a nearly point-like, tetraquark combination consisting of an anticolored diquark and a colored diantiquark in an S -wave and tightly bound by the QCD color force [100, 101] (see Fig. 1c).

Problems with the two above-mentioned pictures have inspired a number of charmonium-molecular hybrid models,⁶ in which the $X(3872)$ is a quantum mechanical mixture of $c\bar{c}$, $D^0\bar{D}^{*0}$ and D^+D^{*-} components [102, 103, 104], where the $c\bar{c}$ component is (mostly) the χ'_{c1} . Hadronic production and radiative transitions to the ψ' and J/ψ are hypothesized to proceed via the $c\bar{c}$ component and this could explain why $X(3872)$ production properties are similar to those of the ψ' and its decay width to $\gamma\psi'$ is larger than that for $\gamma J/\psi$ (because of the closer overlap of the χ'_{c1} and ψ' radial wavefunctions).

Friedmann eschews potential model ideas for meson spectra entirely, including the notion of radial excited states and manages to reproduce the entire spectrum of measured meson and baryon states, including the XYZ meson candidates, with a uniform picture that is based only on quarks and diquarks [105].

In the following I compare molecule, QCD-tetraquark and “hybrid” models to measurements. (I have no comments on Friedmann’s unified model because no phenomenological consequences are currently available.)

4.4.1 A molecule?

The spatial extent of a $D^0\bar{D}^{*0}$ “molecule” with the $X(3872)$ mass would be characterized by its scattering length $a_0 = \hbar/\sqrt{\mu\delta E_0}$ [106], where $\mu = 970$ MeV is the $D\bar{D}^*$ reduced mass and $\delta E_0 \equiv |M_{X(3872)} - (m_{D^0} + m_{D^{*0}})| = 0.003 \pm 0.192$ MeV [95]. The close proximity of the $X(3872)$ mass to the $m_{D^0} + m_{D^{*0}}$ threshold implies a characteristic size of the $D^0\bar{D}^{*0}$ system of $a_0 > 10$ fm, *i.e.*, more than ten times the rms radius of the ψ' , $\langle r_{\psi'} \rangle \sim 0.8$ fm [88, 107]. In contrast, $\delta E_{\pm} \equiv |M_{X(3872)} - (m_{D^+} + m_{D^{*-}})| = 8.2 \pm 0.2$ MeV [21], and $a_{\pm} \sim 2$ fm. This $D^0\bar{D}^{*0}$ - D^+D^{*-} difference easily accounts for the strong isospin violations in $X(3872)$ decays. On the other hand, it is hard to imagine that such a large, weakly bound system would be produced in ultra-high energy $\bar{p}p$ collisions with a cross section and production properties that so closely match those of the compact and tightly bound ψ' charmonium state. In fact, a detailed examination [108] confirms this intuitive expectation and shows that a $D\bar{D}^*$ molecule-like structure could not be promptly produced in high energy hadron collisions with characteristics that are in any way similar to those for the ψ' .

⁶This “hybrid” is not the same as the QCD hybrid shown in Fig. 1d.

Another problem with a purely molecular picture for the $X(3872)$ is the above-mentioned result $\mathcal{B}(X(3872) \rightarrow \gamma\psi') = (2.5 \pm 0.7) \times \mathcal{B}(X(3872) \rightarrow \gamma J/\psi)$. In specific molecule models, $\gamma\psi'$ decays are suppressed relative to $\gamma J/\psi$ by more than two orders of magnitude [109].

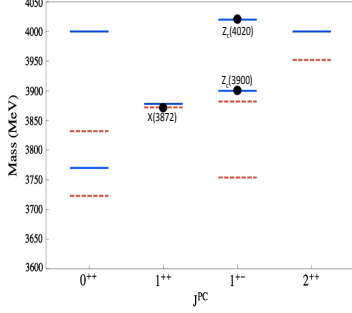


Figure 6: Predicted diquark-diantiquark S -wave states from Ref. [110] (blue lines), with black dots indicating the levels assigned to the $X(3872)$, $Z_c(3900)$ and $Z_c(4020)$. Red dashes show an earlier version of the model [100].

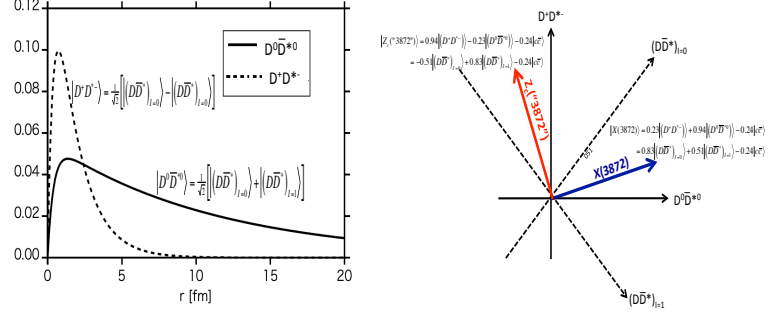


Figure 7: **Left** The radial wave functions for the $D^0\bar{D}^{*0}$ (solid curve) and $D^+\bar{D}^{*-}$ (dashed curve) components of the $X(3872)$ in the charmonium-molecule hybrid model of Ref. [103]. **Right** The blue arrow indicates the isospin components of the $X(3872)$ state vector given in Ref. [103]. The red arrow is the orthogonal (mostly isovector) counterpart of the $X(3872)$ (assuming equal $c\bar{c}$ components).

4.4.2 A QCD tetraquark?

In the diquark-diantiquark picture, a charmoniumlike tetraquark has a $cq_i\bar{c}\bar{q}_j$ configuration, where $q_{1(2)} = u(d)$. For the $X(3872)$, $i = j$ and two configurations are expected: either $cu\bar{c}\bar{u}$ and $cd\bar{c}\bar{d}$ or linear combinations of the two [100, 110]. In addition to two neutral states, two charged states, where $i \neq j$ are also expected. Searches for nearby neutral [39] and charged [33, 111] partners of the $X(3872)$ have come up empty. This model predicts the existence of S -wave diquark-diantiquark states with $J^{PC} = 0^{++}, 1^{+-}$ and 2^{++} , as indicated in Fig. 6. The recently discovered $Z_c(3900)$ and $Z_c(4020)$ are identified as the expected 1^{+-} states, although the initial version of the model, shown as dashed red lines, specifically predicted that the $Z_c(4020)$ mass would be lower, and not higher, than $M_{Z_c(3900)}$ [112]. Many predicted states remain unseen, including a 0^{++} state with a mass that is close to the $D\bar{D}$ open-charmed threshold, which suggests that it might be narrow and relatively easy to see. Note that all of the indicated levels correspond to isospin triplets, so, if this model is correct, lots of additional states remain to be found.

4.4.3 A $c\bar{c}$ - $D\bar{D}^*$ “hybrid?”

The $c\bar{c}$ - $D\bar{D}^*$ hybrid model accommodates the measured properties of the $X(3872)$, including large isospin violations, production properties in high energy $p\bar{p}$ collisions, and the relatively large $\gamma\psi'$ decay width. In a specific version of this model, the authors of Ref. [103] introduce both a mutual interaction between the D and \bar{D}^* and a coupling between the $c\bar{c}$ “core” and $D\bar{D}^*$ systems. This results in a $X(3872)$ state vector of the form:

$$|X(3872)\rangle = \alpha_0|D^0\bar{D}^{*0}\rangle + \alpha_{\pm}|D^+\bar{D}^{*-}\rangle + \alpha_{\text{core}}|c\bar{c}\rangle. \quad (4.1)$$

Because of the disparate mass differences between the $X(3872)$ and the $D^0\bar{D}^{*0}$ and D^+D^{*-} thresholds, the amplitudes and wave functions of these two components are quite different, as shown for a specific example in the left-hand panel of Fig. 7. This means $\alpha_0 \neq \alpha_{\pm}$ and, thus, an $X(3872)$ state with mixed isospin:

$$|X(3872)\rangle = \frac{\alpha_0 + \alpha_{\pm}}{\sqrt{2}} |(D\bar{D}^*)_{I=0}\rangle + \frac{\alpha_0 - \alpha_{\pm}}{\sqrt{2}} |(D\bar{D}^*)_{I=1}\rangle + \alpha_{\text{core}} c\bar{c}. \quad (4.2)$$

In the Ref. [103] calculation, $\alpha_0 = 0.94$, $\alpha_{\pm} = 0.23$ and $\alpha_{\text{core}} = -0.24$, corresponding to probabilities of 68% for $I = 0$, 25% for $I = 1$ and 6% for the $c\bar{c}$ core. An interesting feature of the Ref. [103] calculation is that the bulk of the attraction between the D and \bar{D}^* mesons in the $X(3872)$ comes from the $c\bar{c}$ - $D\bar{D}^*$ coupling. The mutual D - \bar{D}^* attraction, which is the dominant term in pure molecular models, only plays a minor role. Similar conclusions are reported in Ref. [104].

The state vector given in Eq. (4.2) has two related orthogonal counterparts. Reference [103] discusses one that is mostly $c\bar{c}$ and probably should be considered to be the physical manifestation of the χ'_{c1} charmonium state. This is found to have a mass that is well above both the $D^0\bar{D}^{*0}$ and D^+D^{*-} thresholds and wide. As a result, it may not be experimentally easy to identify. The third state would be predominantly a $D\bar{D}^*$ isovector with a large D^+D^{*-} component, as illustrated in the right-hand panel of Fig. 7.⁷ If this is a physical particle, it might be accessible in $B \rightarrow K D\bar{D}^*$ decays. The near-threshold $M(D^0\bar{D}^{*0})$ distributions for $B \rightarrow K D^0\bar{D}^{*0}$ published by Belle [43] and Babar [44] have limited statistics and are inconclusive (see, *e.g.*, Fig. 3c). To date, no results for charged $(D\bar{D}^*)^+$ combinations have been published.

5. The charged Z mesons

5.1 The Z(4430)

Figure 8a shows the $M(\pi^+\psi')$ distribution for $B \rightarrow K\pi^+\psi'$ decays reported by Belle in 2007 [77]. Here, to reduce the influence of the dominant $B \rightarrow K^*(890)\psi'$ and $K_2^*(1430)\psi'$ decay channels, events with $K\pi$ invariant masses within ± 100 MeV of the $K^*(890)$ or $K_2^*(1430)$ peaks have been excluded (the “ K^* veto”). The distinct peak is fitted with a Breit-Wigner (BW) resonance on an incoherent background. The BW signal from the fit has a statistical significance of $\sim 8\sigma$, with a mass and width of $M = 4433 \pm 5$ MeV and $\Gamma = 45^{+35}_{-18}$ MeV. Since this peak structure has a non-zero electrical charge, if it is due to a meson resonance, that meson must necessarily have a minimal $c\bar{c}u\bar{d}$ four-quark substructure.

A BaBar study of the $B \rightarrow K\pi^+\psi'$ decay channel did not confirm the Belle result [113]. A (nearly) direct comparison of the Belle and BaBar results for $M(\pi^+\psi')$ from $B \rightarrow K\pi^+\psi'$ with a K^* veto is shown in Fig. 8b. Although the BaBar plot shows an excess of events in the same $M(\pi^+\psi')$ region as the Belle signal, their fit using Belle’s mass and width values yielded a statistically marginal ($\sim 2\sigma$) $Z(4430) \rightarrow \pi^+\psi'$ signal. Belle responded to concerns about the possibility of $M(\pi^+\psi')$ reflection peaks due to interference between different partial waves in the $K\pi$ resonance channels by doing two different coherent amplitude analyses of the $B \rightarrow K\pi^+\psi'$ decay process. The first one used coherent amplitudes that depended on two kinematic variables ($M(K\pi^+)$

⁷This state would be distinct from the $Z_c(3900)$ because of its opposite C -/ G -parity.

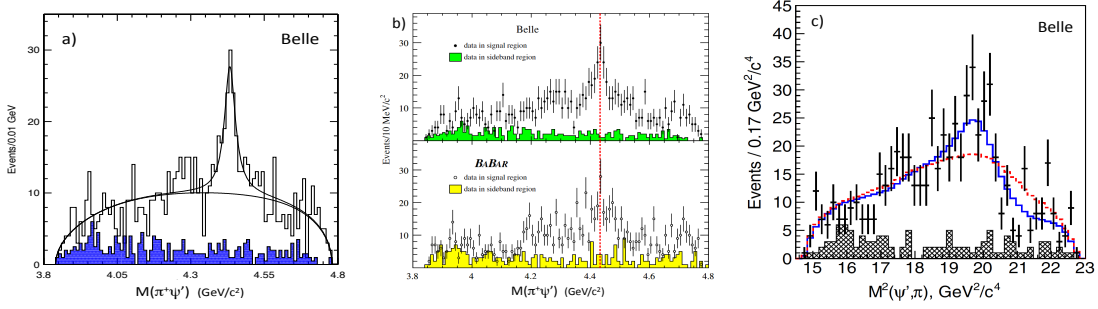


Figure 8: a) The $\pi^+\psi'$ invariant mass distribution from $B \rightarrow K\pi^+\psi'$ decays from Belle [77] for events with the K^* veto requirement applied is shown as the open histogram. The shaded histogram is non- ψ' background, estimated from the ψ' mass sidebands. The curves represent results of a fit that returned the mass and width values quoted in the text. b) A comparison of Belle (*upper*) and BaBar (*lower*) data [113] with the K^* and K_2^* vetoed. c) The data points show the Belle $M^2(\pi^+\psi')$ distribution with the K^* veto applied. The solid blue histogram shows a projection of the Belle 4D fit results with a $Z^+ \rightarrow \pi^+\psi'$ resonance included [79]. The dashed red curve shows fit results with no resonance in the $\pi^+\psi'$ channel.

and $M(\pi^+\psi')$ [78] and the second one used kinematically complete four-dimensional (4D) amplitudes that incorporated possible dependence on the $\psi' \rightarrow \ell^+\ell^-$ decay helicity angle and the angle between the $K\pi^+$ and $\psi' \rightarrow \ell^+\ell^-$ decay planes [79]. Both reanalyses, which included all known $K\pi$ resonances and allowed for contributions from possible additional ones, confirmed the existence of a resonance in the $\pi^+\psi'$ channel with greater than 6σ significance, but with larger mass and width values than those from Belle's original analysis [77]: the results from the 4D analyses are $M = 4485^{+36}_{-25}$ MeV and $\Gamma = 200^{+48}_{-58}$ MeV.

The reason for the upward shifts in mass and width from Belle's originally published results can be seen in Fig. 8c, which shows a comparison of projections of the 4D fit results with the experimental $M^2(\pi^+\psi')$ distribution with the K^* veto applied. The dashed red histogram shows the best fit results with no resonance in the $\pi^+\psi'$ channel. The solid blue histogram shows results with the inclusion of a single $\pi^+\psi'$ resonance, where strong interference effects that are constructive below, and destructive above, the resonance mass, are evident. The original Belle analysis neglected interference effects and only fitted the lower lobe of this double-lobed interference pattern, and this resulted in a lower mass and narrower width.

5.1.1 LHCb confirmation of the $Z(4430)$

The big news in 2014 was the confirmation of the Belle $Z(4430) \rightarrow \pi^+\psi'$ claims by the LHCb experiment [80] based on a data sample containing $\sim 25K$ $B^0 \rightarrow K^-\pi^+\psi'$ events, an order of magnitude larger than the event samples used by either Belle or BaBar. They find that their $M(\pi^+\psi')$ mass distribution cannot be reproduced by reflections from the $K\pi$ channel either with a model-dependent assortment of $K\pi$ resonances up to $J=3$, or by a model-independent approach that determines Legendre polynomial moments up to fourth order ($J_{K^*} \leq 2$) in $\cos\theta_{K^*}$ in bins of $K\pi$ mass, where θ_{K^*} is the $K\pi$ helicity angle, and reflects them into the $\pi^+\psi'$ channel. Figure 9a shows a comparison of the $M(\pi^+\psi')$ data with a fit that only uses reflections from the $\cos\theta_{K^*}$ moments, where a clear discrepancy shows up in the $Z(4430)$ mass region. The application of the Belle 4D amplitude analysis procedure that includes a BW resonance amplitude in the $\pi^+\psi'$ channel

results in a $Z(4430)$ signal with a huge, $\sim 14\sigma$, statistical significance and mass & width values ($M = 4475_{-26}^{+17}$ MeV & $\Gamma = 172_{-36}^{+39}$ MeV) that are in close agreement with the Belle 4D analysis results. A comparison of the LHCb fit results with the data is shown in Fig. 9b, where strong interference effects, similar to those seen by Belle (Fig. 8c), are evident.

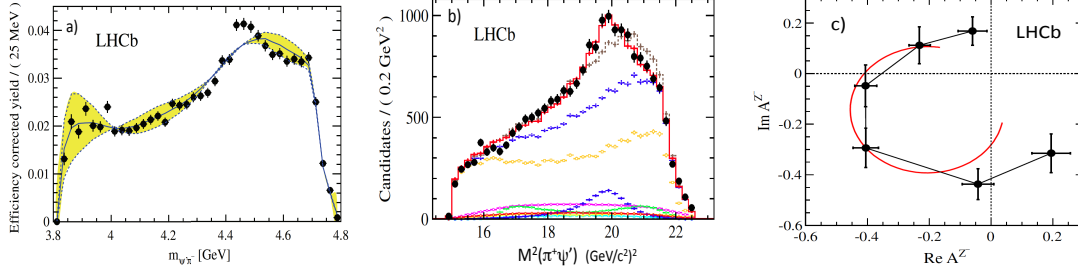


Figure 9: **a)** The data points show LHCb’s background-subtracted and efficiency corrected $M(\pi^+\psi')$ distribution. The solid blue curve shows the result of the fit using model-independent reflections from $\cos\theta_{K^*}$ moments up to fourth-order. The shaded band indicates the range of errors associated with the fit. **b)** The LHCb $M^2(\pi^+\psi')$ distribution for all events (no K^* veto), together with projections from the four-dimensional fits. The solid red histogram shows the fit that includes a $Z^+ \rightarrow \pi^+\psi'$ resonance term; the dashed brown histogram shows the fit with no resonance in the $\pi^+\psi'$ channel. **c)** The Real (horizontal) and Imaginary (vertical) parts of the (1^+) $Z^+ \rightarrow \pi^+\psi'$ amplitude for six mass bins spanning, counter-clockwise, the 4430 MeV mass region (from LHCb [80]). The red curve shows expectations for a BW resonance amplitude.

The LHCb group’s large data sample enabled them to relax the assumption of a BW form for the $Z^+ \rightarrow \pi^+\psi'$ amplitude and directly measure the real and imaginary parts of the $1^+ \pi^+\psi'$ amplitude in bins of $\pi^+\psi'$ mass. The results are shown as data points in the Argand plot in Fig. 9c. There, the phase motion near the resonance peak agrees well with expectations for a BW amplitude as indicated by the circular red curve superimposed on the plot. This rapid phase motion near amplitude-maximum is characteristic of a BW-like resonance. (The orientation of the red circle reflects the phase angle between the $B \rightarrow KZ$ and $B \rightarrow K^*(890)\psi'$ decay amplitudes.)

The weighted averages of the LHCb and Belle mass and width measurements are $M_{Z(4430)} = 4477 \pm 20$ MeV and $\Gamma_{Z(4430)} = 181 \pm 31$ MeV. This mass is near $(m_D + m_{D(2600)}) = 4479 \pm 6$ MeV, where the $D(2600)$ is a candidate for the $D^*(2S)$, the first radial excitation of the D^* , that was reported by BaBar in 2010 [114].

5.1.2 The recently discovered $Z_c(4200)$ and observation of $Z(4430) \rightarrow \pi^+ J/\psi$

New at this meeting are results from a Belle 4D amplitude analysis of $B^0 \rightarrow K^- \pi^+ J/\psi$ decays [76], based on a nearly background-free data sample containing $\simeq 30K$ events. The main result from this analysis is a 6.2σ signal for a broad $\pi^+ J/\psi$ resonance, dubbed the $Z_c(4200)$, with mass and width $M = 4196_{-29}^{+31} {}_{-13}^{+17}$ MeV and $\Gamma = 370_{-70}^{+70} {}_{-132}^{+70}$ MeV, and a preferred quantum number assignment of $J^P = 1^+$. Figure 10a shows Belle’s $M^2(\pi^+ J/\psi)$ distribution for events with $K\pi$ masses that lie between the $K^*(890)$ and $K_2^*(1432)$ resonance regions, with a projection from the best fit for a model in which the $Z(4430)$ (with mass and width set at the Ref. [79] values) is the only resonance in the $\pi^+ J/\psi$ channel (dashed red histogram) and results from a fit that includes an additional $\pi^+ J/\psi$ resonance (solid blue histogram). Figure 10b shows similar results for events with $K\pi$ masses above the $K_2^*(1432)$ resonance region. Figure 10c shows an Argand plot for

the (dominant) Helicity=1, $J^P = 1^+$ $\pi^+ J/\psi$ amplitude in the 4200 MeV mass region, where rapid phase motion near 4200 MeV is evident. The LHCb group [80] reported evidence for a broad $\pi^+ \psi'$ resonance in this mass region with $J^P = 0^-$ or 1^+ , which may be an indication of a $\pi^+ \psi'$ decay mode of the $Z_c(4200)$. There are no open-charmed meson-antimeson combinations that could form a 1^+ S -wave resonance with a mass threshold that are within $\sim \pm 100$ MeV of the $Z_c(4200)$, which speaks against a molecule-like interpretation for this peak.

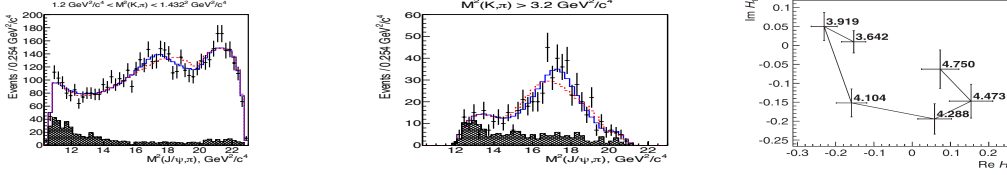


Figure 10: **a)** The data points show Belle’s $M^2(\pi^+ J/\psi)$ distribution for $B^0 \rightarrow K^- \pi^+ J/\psi$ events with $M(K\pi)$ between the $K^*(890)$ and $K_2^*(1432)$ resonance regions. The dashed red histogram shows the projection of the results of a fit with no resonances in the $\pi J/\psi$ channel and solid blue histogram is the projection of the fit that includes $Z_c(4200)$ and $Z(4430)$ BW amplitudes. **b)** The $M^2(\pi^+ J/\psi)$ distribution for events with $M(K\pi)$ above the $K_2^*(1432)$ resonance region. The histograms are fit projections with and without Z resonance amplitudes. **c)** The Real (horizontal) and Imaginary (vertical) parts of the 1^+ zero-helicity $Z^+ \rightarrow \pi^+ J/\psi$ amplitude for six mass bins spanning the 4200 MeV mass region (from Belle [76]).

The Belle $B^0 \rightarrow K^- \pi^+ J/\psi$ analysis also found a 4σ signal for $B^0 \rightarrow K^- Z(4430)^+; Z(4430)^+ \rightarrow \pi^+ J/\psi$ with a product branching fraction

$$\mathcal{B}(B^0 \rightarrow K^- Z(4430)^+) \times \mathcal{B}(Z(4430)^+ \rightarrow \pi^+ J/\psi) = 5.4_{-1.0}^{+4.0} {}_{-0.9}^{+1.1} \times 10^{-6}, \quad (5.1)$$

which is an order of magnitude smaller (albeit with large errors) than the corresponding value for $B^0 \rightarrow K^- Z(4430)^+; Z(4430)^+ \rightarrow \pi^+ \psi'$ decays: $6.0_{-2.9}^{+1.7} {}_{-4.9}^{+2.5} \times 10^{-5}$. A search for $B^0 \rightarrow K^- Z_c(3900)^+; Z_c(3900)^+ \pi^+ J/\psi$ found no signal; a product branching fraction upper limit of $< 9 \times 10^{-7}$ (90% CL) was established.

5.2 The $Z_c(3900)$ and $Z_c(4020)$

The discovery and early measurements of the $Y(4260)$ were based on measurements of the initial state radiation process, $e^+ e^- \rightarrow \gamma_{\text{ISR}} Y(4260)$ at $E_{\text{cm}} \simeq 10.6$ GeV. This reaction requires that either the incident e^- or e^+ radiates a ~ 4.5 GeV photon prior to annihilating, which results in a strong reduction in event rate. However, since the PEP-II and KEKB B -factories ran with such high luminosities ($\mathcal{L} > 10^{34} \text{ cm}^{-2} \text{ s}^{-1}$), the measurements were feasible. A more efficient way to produce $Y(4260)$ mesons would be to operate a high luminosity $e^+ e^-$ collider as a “ $Y(4260)$ factory,” *i.e.*, at a cm energy of 4260 MeV, corresponding to the peak mass of the $Y(4260)$. This was done at the two-ring Beijing electron-positron collider (BEPC-II) [115] in 2013, and large numbers of $Y(4260)$ decays were detected in the BES-III spectrometer [116]. This resulted in the discoveries of two additional charged charmoniumlike states: the $Z_c(3900)$ and $Z_c(4020)$.

5.2.1 The $Z_c(3900)$

The first channel to be studied with the $E_{\text{cm}} = 4260$ MeV data was $e^+ e^- \rightarrow \pi^+ \pi^- J/\psi$, where a distinct peak, called the $Z_c(3900)$, was seen near 3900 MeV in the distribution of the larger of the

two $\pi^\pm J/\psi$ invariant mass combinations in each event ($M_{\max}(\pi J/\psi)$), as can be seen shown in Fig. 11a [68]. A fit using a mass-independent-width BW function to represent the $\pi^\pm J/\psi$ mass peak yielded a mass and width of $M_{Z_c(3900)} = 3899.0 \pm 6.1$ MeV and $\Gamma_{Z_c(3900)} = 46 \pm 22$ MeV, which is ~ 24 MeV above the $m_{D^{*+}} + m_{\bar{D}^0}$ (or $m_{D^+} + m_{\bar{D}^{*0}}$) threshold. The $Z_c(3900)$ was observed by Belle in isr data at the same time [69].

A subsequent BESIII study of the $(D\bar{D}^*)^+$ systems produced in $(D\bar{D}^*)^\pm \pi^\mp$ final states in the same data sample, found very strong near-threshold peaks in both the $D^0 D^{*-}$ and $D^+ \bar{D}^{*0}$ invariant mass distributions [70], as shown in Fig. 11b. The curves show results of fits to the data with threshold-modified BW line shapes to represent the peaks. The average values of the mass and widths from these fits are used to determine the resonance pole position ($M_{\text{pole}} + i\Gamma_{\text{pole}}$) with real and imaginary values of $M_{\text{pole}} = 3883.9 \pm 4.5$ MeV and $\Gamma_{\text{pole}} = 24.8 \pm 12$ MeV.

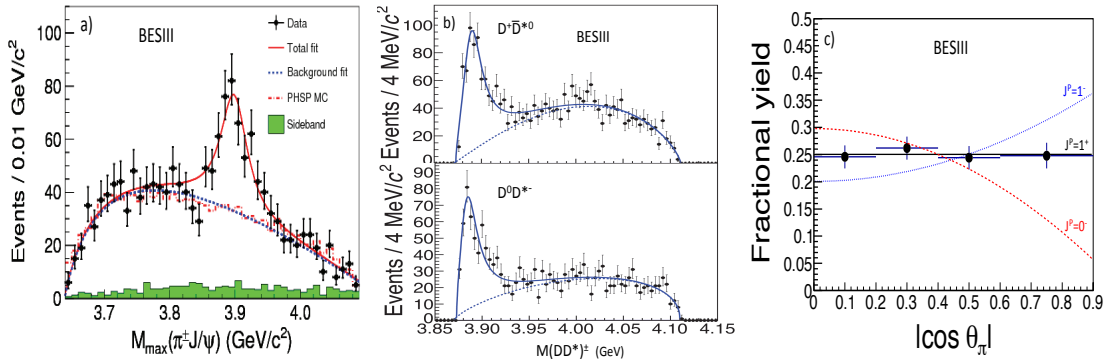


Figure 11: a) Invariant mass distributions for $\pi^\pm J/\psi$ from $e^+e^- \rightarrow \pi^+ \pi^- J/\psi$ events from Ref. [68]; b) $M(D^+ \bar{D}^{*0})$ (top) and $M(D^0 D^{*-})$ (bottom) for $e^+e^- \rightarrow (D\bar{D}^*)^\pm \pi^\mp$ events from Ref. [70]; c) the efficiency corrected production angle distribution compared with predictions for $J^P = 0^-$ (dashed-red), $J^P = 1^-$ (dotted blue) and $J^P = 1^+$ (solid black) quantum number assignments.

Since the pole mass position is $\simeq 2\sigma$ lower than the $Z_c(3900)$ mass reported in Ref. [68], BESIII cautiously named this $D\bar{D}^*$ state the $Z_c(3885)$. In the mass determinations of both the $Z_c(3885)$ and $Z_c(3900)$, effects of possible interference with a coherent component of the background are ignored, which can bias the measurements by amounts comparable to the resonance widths, and this might account for the different mass values. In any case, we consider it highly likely that the $Z_c(3885)$ is the $Z_c(3900)$ in a different decay channel. If this the case, the partial width for $Z_c(3900) \rightarrow D\bar{D}^*$ decays is 6.2 ± 2.9 times larger than that for $J/\psi \pi^+$, which is small compared to open-charm vs. hidden-charm decay-width ratios for established charmonium states above the open-charm threshold, such as the $\psi(3770)$ and $\psi(4040)$, where corresponding ratios are measured to be more than an order-of-magnitude larger [21].

Since the $Z_c(3885) \rightarrow D\bar{D}^*$ signals are so strong, the J^P quantum numbers could be determined from the dependence of its production on θ_π , the polar angle of the bachelor-pion track relative to the beam direction in the e^+e^- cm system. For $J^P = 0^-$, $dN/d|\cos \theta_\pi|$ should go as $\sin^2 \theta_\pi$; for 1^- it should follow $1 + \cos^2 \theta_\pi$ and for 1^+ it should be flat (0^+ is forbidden by Parity). Figure 11c shows the efficiency-corrected $Z_c(3885)$ signal yield as a function of $|\cos \theta_\pi|$, together with expectations for $J^P = 0^+$ (dashed red), 1^- (dotted blue) and $J^P = 1^+$. The $J^P = 1^+$ assignment is clearly preferred and the 0^- and 1^- assignments are ruled out with high confidence.

5.2.2 The $Z_c(4020)$

With data accumulated at the peaks of the $Y(4260)$, $Y(4360)$ and nearby energies, BESIII made a study of $\pi^+\pi^-h_c(1P)$ final states. The exclusive $h_c(1P)$ decays were detected via the $h_c \rightarrow \gamma\eta_c$ transition, where the η_c was reconstructed in 16 exclusive hadronic decay modes. With these data, BESIII observed a distinct peak near 4020 MeV in the $M_{\max}(\pi^\pm h_c)$ distribution that is shown in Fig. 12a. A fit to this peak, which the BESIII group called the $Z_c(4020)^+$, with a signal BW function (assuming $J^P = 1^+$) plus a smooth background, returns a $\sim 9\sigma$ significance signal with a fitted mass of $M_{Z_c(4020)} = 4022.9 \pm 2.8$ MeV, about 5 MeV above $m_{D^{*+}} + m_{\bar{D}^{*0}}$, and a width of $\Gamma_{Z_c(4020)} = 7.9 \pm 3.7$ MeV [71]. The product $\sigma(e^+e^- \rightarrow \pi^- Z_c(4020)^+) \times \mathcal{B}(Z_c(4020)^+ \rightarrow \pi^+ h_c)$ is measured to be $7.4 \pm 2.7 \pm 1.2$ pb at $E_{\text{cm}} = 4260$ MeV, where the second error reflects the uncertainty of $\mathcal{B}(h_c \rightarrow \gamma\eta_c)$.

The inset in Fig. 12a shows the result of including a $Z_c(3900)^+ \rightarrow \pi^+ h_c$ term in the fit. In this case, a marginal $\sim 2\sigma$ signal for $Z_c(3900)^+ \rightarrow \pi^+ h_c$ is seen to the left of the $Z_c(4020)$ peak. This translates into an upper limit on the product $\sigma(e^+e^- \rightarrow \pi^- Z_c(3900)^+) \times \mathcal{B}(Z_c(3900)^+ \rightarrow \pi^+ h_c)$ of 11 pb. Since the product $\sigma(e^+e^- \rightarrow \pi^- Z_c(3900)^+) \times \mathcal{B}(Z_c(3900)^+ \rightarrow \pi^+ J/\psi)$ is measured to be 62.9 ± 4.2 pb [68], this limit implies that the $Z_c(3900)^+ \rightarrow \pi^+ h_c$ decay channel is suppressed relative to that for $\pi^+ J/\psi$ by at least a factor of five.

BESIII recently reported observation of the neutral member of the $Z_c(4020)$ isospin triplet [73]. The $M_{\max}(\pi^0 h_c)$ distribution for $e^+e^- \rightarrow \pi^0 \pi^0 h_c$ events in the same data set, shown in Fig. 12b, looks qualitatively like the $M_{\max}(\pi^+ h_c)$ distribution with a distinct peak near 4020 MeV. A fit to the data that includes a BW term with a width fixed at the value measured for the $Z_c(4020)^+$ and floating mass returns a mass of 4023.9 ± 4.4 MeV; this and the signal yield are in good agreement with expectations based on isospin symmetry.

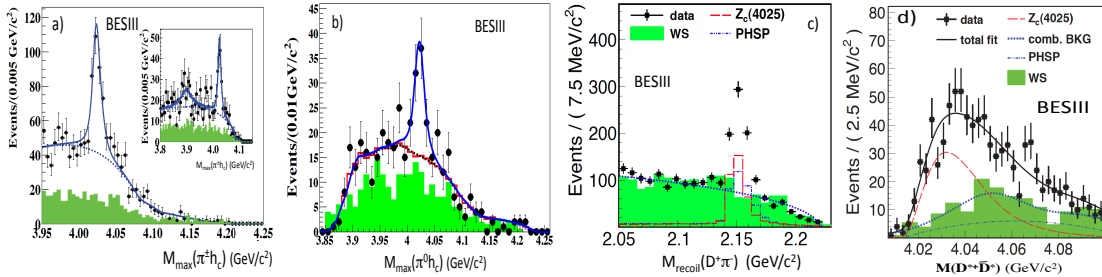


Figure 12: **a)** The $M_{\max}(\pi^+ h_c)$ distribution for $e^+e^- \rightarrow \pi^+\pi^-h_c$ events from BESIII. The shaded histogram is background estimated from the h_c mass sidebands. The curves are results of fits described in the text. **b)** The corresponding $M_{\max}(\pi^0 h_c)$ distribution for $e^+e^- \rightarrow \pi^0\pi^0 h_c$ events from BESIII. **c)** The distribution of masses recoiling from a detected D^+ and π^- for $e^+e^- \rightarrow D^+\pi^-\pi^0 X$ events at $\sqrt{s} = 4260$ MeV. The peak near 2.15 MeV corresponds to $e^+e^- \rightarrow \pi^- D^{*+} \bar{D}^{*0}$ events. The red dashed histogram shows the expected recoil mass distribution for $e^+e^- \rightarrow \pi^- Z_c$, with $M_{Z_c} = 4025$ GeV; the open, dash-dot histogram shows results for MC $\pi^- D^{*+} \bar{D}^{*0}$ three-body phase-space events. The shaded histogram is combinatoric background from wrong-sign combinations in the data. **d)** $M(D^* \bar{D}^*)$ for $e^+e^- \rightarrow (D^* \bar{D}^*)^+ \pi^-$ events, *i.e.*, events in the 2.25 MeV peak in panel c. The curves are described in the text.

BESIII studied $e^+e^- \rightarrow D^{*+} \bar{D}^{*0} \pi^-$ events in the $E_{\text{cm}} = 4.26$ GeV data sample using a partial reconstruction technique that only required the detection of the bachelor π^- , the D^+ from the $D^{*+} \rightarrow \pi^0 D^+$ decay and one π^0 , either from the D^{*+} or the \bar{D}^{*0} decay, to isolate the process and

measure the $D^{*+}\bar{D}^{*0}$ invariant mass [72]. The signal for real $D^{*+}\bar{D}^{*0}\pi^-$ final states is the distinct peak near 2.15 MeV in the $D^+\pi^-$ recoil mass spectrum shown on Fig. 12c. The measured $D^*\bar{D}^*$ invariant mass distribution for events in the 2.15 MeV peak, shown as data points in Fig. 12d, shows a strong near-threshold peaking behavior with a shape that cannot be described by a phase-space-like distribution, shown as a dash-dot blue curve, or by combinatoric background, which is determined from wrong-sign (WS) events in the data (*i.e.*, events where the bachelor pion and charged D meson have the same sign) that are shown as the shaded histogram. The solid black curve shows the results of a fit to the data points that includes an efficiency weighted S -wave BW function, the WS background shape scaled to measured non- $D^{*+}\bar{D}^{*0}\pi^-$ background level under the signal peak in Fig. 12d, and a phase-space term. The fit returns a 13σ signal with mass and width $M = 4026.3 \pm 4.5$ MeV and $\Gamma = 24.8 \pm 9.5$ MeV, values that are close to those measured for the $Z_c(4020)^+ \rightarrow \pi^+ h_c$ channel. Although BESIII cautiously calls this $(D^*\bar{D}^*)^+$ signal the $Z_c(4025)$, in the following we assume that this is another decay mode of the $Z_c(4020)$.

From numbers provided in Ref. [72], we determine $\sigma(e^+e^- \rightarrow \pi^- Z_c(4020)) \times \mathcal{B}(Z_c(4020) \rightarrow D^*\bar{D}^*) = 89 \pm 19$ pb. This implies that the partial width for $Z_c(4020) \rightarrow D^*\bar{D}^*$ is larger than that for $Z_c(4020) \rightarrow \pi h_c$, but only by a factor of 12 ± 5 , not by the large factors that are characteristic of open charm decays of conventional charmonium.

The J^P values of the $Z_c(4020)^+$ have not been determined. As mentioned in Lange's talk at this meeting, charged bottomoniumlike states have been seen in the b -quark sector just above the $B\bar{B}^*$ and $B^*\bar{B}$ open-bottom thresholds [82], the $Z_b(10610)$ and $Z_b(10650)$, respectively, and both have been determined to have $J^P = 1^+$ [83]. Thus $J^P = 1^+$ is probably a reasonable guess for the $Z_c(4020)$.

5.3 Are there non-resonant sources for the near threshold $Z_c(3900)$ and $Z_c(4020)$ peaks?

The $Z_c(3900)^+$ and the $Z_c(4020)^+$ are just above the $D\bar{D}^*$ and $D^*\bar{D}^*$ thresholds, and the decay modes $Z_c(3900) \rightarrow D\bar{D}^*$ and $Z_c(4020) \rightarrow D^*\bar{D}^*$ have been seen. For Z_c quantum numbers of $J^P = 1^+$, the $D^{(*)}\bar{D}^*$ system are in an S -wave. In this case, the coupled-channel process illustrated in diagram b of Fig. 13 (left), can produce a sharp peaking structure in the $\pi J/\psi$ (h_c) invariant mass distribution just above the $D^{(*)}\bar{D}^*$ threshold.⁸ It has been suggested that the observed Z_c (and Z_b) peaks are not due to genuine mesons, but are, instead, artifacts of this coupled-channel process [117, 118, 119].

5.3.1 Cusps?

The $D\bar{D}^*$ loop in diagram b of Fig. 13 (left) produces an imaginary amplitude that rises rapidly starting at $M(\pi J/\psi) = m_D + m_{\bar{D}^*}$; this rapid rise is subsequently cutoff by a form-factor. The net effect is a cusp-like peaking structure in the $\pi J/\psi$ (h_c) ($\pi\Upsilon$ (h_b)) invariant mass distributions just above the $D\bar{D}^*$ ($B\bar{B}^*$) threshold. The authors of Refs. [118] and [119] claim that these effects can at least qualitatively reproduce the general features of published $Z_c(3900) \rightarrow \pi J/\psi$ data, as shown in the center and right panels of Fig. 13.

⁸The left-most panels of Figs. 13 and 14 apply specifically to the $Z_c(3900)$. Diagrams for the $Z_c(4020) \rightarrow D^*\bar{D}^*$ (and the Z_b) processes are similar.

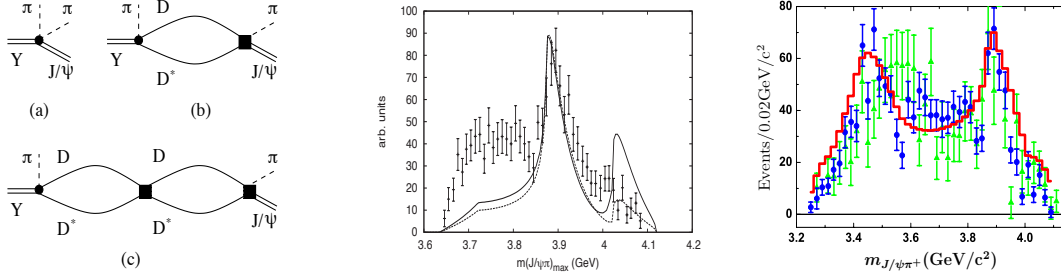


Figure 13: **Left:** (Figure 2 from Ref. [120].) **a)** Tree, **b)** one-loop and **c)** two-loop diagrams for $Y(4260) \rightarrow \pi^+ \pi^- J/\psi$. **Center:** (Figure 6 from Ref. [119].) A comparison of BESIII $M(\pi^+ J/\psi)$ data [68] with the expectations for a cusp induced by a single $D\bar{D}^*$ loop that is cut off with a Gaussian form factor. **Right:** (Figure 2 from Ref. [118].) $M(\pi J/\psi)$ data with results from a fit to a coupled-channel induced cusp produced by a single DD^* loop and cut off with a dipole form-factor, plus a tree diagram with resonances in the $\pi^+ \pi^-$ channel. The round (blue) data points are from BESIII [68] and the triangular (green) data points are from Belle [69].

5.3.2 Non-perturbative effects?

A more detailed study of this effect is discussed in Ref. [120], where it is pointed out that the closely related diagrams shown in Fig. 14 (left), with the same form-factor and the same $Y-\pi D\bar{D}^*$ coupling, apply to the $Z_c \rightarrow D\bar{D}^*$ channel, where they can produce threshold enhancements such as the $Z_c(3900) \rightarrow D\bar{D}^*$ structure reported by BESIII [70]. The solid red curve in Fig. 14 (center) shows results of a Ref. [120] fit to the BESIII $M(D\bar{D}^*)$ distribution that includes the tree and single $D\bar{D}^*$ loop terms (diagrams a and b in Fig. 14(left)), and cut off by a Gaussian form-factor; this fit shows that reasonable agreement with the data is possible. The solid red curve in Fig. 14 (right) shows the results of a subsequent Ref. [120] fit to the $M(\pi J/\psi)$ data from BESIII with the tree and single DD^* loop diagrams of Fig. 13 (left), for which the values of the $Y-\pi D\bar{D}^*$ coupling and the width of the Gaussian form-factor are fixed at their $M(D\bar{D}^*)$ -fit values. Although the fit quality here is poorer, the $Z_c(3900) \rightarrow \pi J/\psi$ peak is at least qualitatively reproduced. (The dashed green lines in the $M(D\bar{D}^*)$ and $M(\pi J/\psi)$ plots show results from fits that only use the tree diagram.)

It is emphasized in Ref. [120] that the comparisons with data shown in the center and right panels of Figs. 13 and 14 are based on only the first two terms of a perturbation series, *i.e.*, diagrams a and b in the left-hand panels of Figs. 13 and 14, and neglect contributions from the double-loop terms shown in diagrams c of the same figures as well as (not shown) three- and higher loop terms. The dashed magenta curves in the center and right panels of Fig. 14 show the effects of adding the double-loop amplitudes based on the parameters determined from the single-loop-only fits. Here dramatic departures from the single-loop-only fit results for both the $M(D\bar{D}^*)$ and $M(\pi J/\psi)$ distributions demonstrate that the neglect of the higher-order terms in the perturbation series, which is implicit in the characterizations given in Refs. [117, 118, 119], is not justified. The dash-dot black curve in the $M(D\bar{D}^*)$ plot of Fig. 14 (center) shows the result of an attempt to fit the $M(D\bar{D}^*)$ distribution with a full perturbation expansion that is forced to converge; here the agreement with data is poor.

Based on these results, the authors of Ref. [120] conclude that the near-threshold Z_c (and Z_b peaks) cannot be purely kinematic effects and must be due to the influence of a nearby pole in the S -matrix, thereby qualifying them as legitimate meson states.

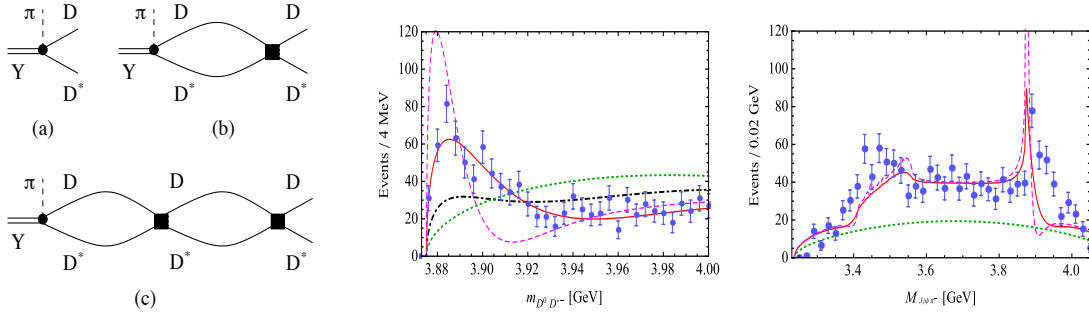


Figure 14: **Left:** **a)** Tree, **b)** one-loop and **c)** two-loop diagrams for $Y(4260) \rightarrow \pi D \bar{D}^*$. (Figure 1 from Ref. [120].) **Center:** The solid (red) curve shows the Ref. [120] fit to the BESIII $M(D\bar{D}^*)$ distribution [70] using the tree and single $D\bar{D}^*$ loop (diagrams a and b in the left panel of this figure) cut off with a Gaussian form factor. The dashed magenta curve includes the two-loop term (diagram c) and the dot-dash black curve shows results when the perturbative expansion is forced to converge. (Figure 3 from Ref. [120].) **Right:** The corresponding fit results applied to the BESIII $M(\pi J/\psi)$ data. (Figure 4 from Ref. [120].)

5.3.3 Experimental tests

The question of whether the near-threshold $Z_{c(b)}$ peaks seen by BESIII and Belle are due to genuine meson states or, instead, coupled-channel kinematic effects is too important to be left to theorists⁹ and should be settled, if possible, by experiment. To date, the BESIII group has only done separate fits to the $M(\pi J/\psi)$ and $M(D\bar{D}^*)$ distributions for their $Z_c(3900) \rightarrow \pi J/\psi$ and $D\bar{D}^*$ data samples. Simultaneous fits using amplitudes suggested in refs. [117, 118, 119, 120] would probably be instructive. More critical would be phase measurements of the $Z_{c(b)}$ amplitudes.

The cusp models discussed above start with imaginary amplitudes generated by the loop diagrams shown in the left panels of Figs. 13 and 14; the real parts of these amplitudes can be determined by analyticity requirements. The resulting phase motion, described in some detail in Ref. [117], is different than that of a BW amplitude. Figure 15a shows the real and imaginary amplitudes and the modulus for a coupled-channel-generated peak from Ref. [119]; Fig. 15b shows a sketch of its associated Argand plot, where the arrow indicates the location of the peak. For comparison, Fig. 15c shows the modulus and phase of a BW resonance, and 15d shows its associated Argand plot. The latter two plots show that the BW amplitude has a rapid, 180° phase change across the resonance peak; this is not the case for the coupled-channel-generated peak, which has a relatively small phase motion surrounding the peak. Thus, with sufficient statistics, amplitude analyses of the $Z_c(3900) \rightarrow \pi J/\psi$ and $D\bar{D}^*$ peaks should be able to distinguish coupled-channel effects from a genuine resonance. The BESIII group is currently doing a Partial Wave Analysis of existing $Z_c(3900) \rightarrow \pi J/\psi$ data that could address this question, albeit with limited statistics [123]. There is also a proposal within the BESIII collaboration to accumulate a much larger $Y(4260) \rightarrow \pi^+ \pi^- J/\psi$ data sample that could be suitable for a definitive distinction between a resonance and coupled-channel-cusp origin for the observed peaks [124].

⁹The theoretical situation remains unclear. Three months after this presentation, Swanson [121] posted a rebuttal to the claims in Ref. [120]. Shortly after that, the Ref. [120] authors responded with a rebuttal to Swanson's rebuttal [122].

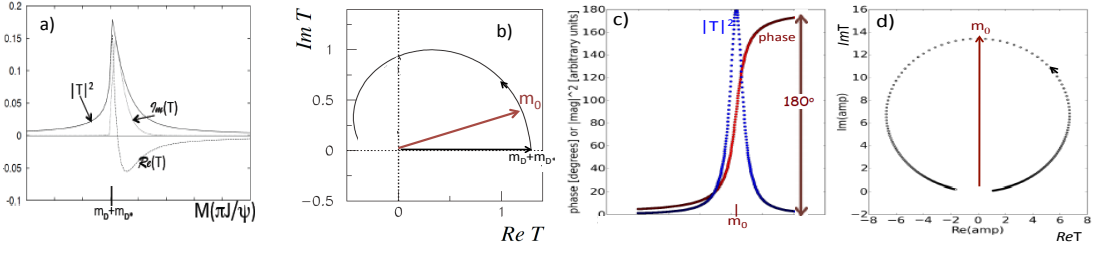


Figure 15: **a)** The real, imaginary and modulus squared for a $D\bar{D}^*$ -loop-generated peak in the $\pi J/\psi$ mass distribution (adapted from Ref. [119]). **b)** A sketch of the Argand diagram generated from the amplitudes shown in a), with the peak location indicated by an arrow (adapted from Ref. [117]). **c)** The modulus and phase of a Breit Wigner resonance. **d)** The Argand plot for a Breit Wigner resonance.

6. Comments and speculations

6.1 Comment on the partial widths for $Z_{(c)} \rightarrow \pi(c\bar{c})$

For standard $c\bar{c}$ mesons, the decay partial widths for hadronic transitions between different charmonium states are typically of order of a few hundreds of keV or less. The largest measured one is $\Gamma(\psi(4040) \rightarrow \eta J/\psi) = 416 \pm 76$ keV; others are smaller, *e.g.*, $\Gamma(\psi' \rightarrow \pi^+ \pi^- J/\psi) = 157 \pm 5$ keV, $\Gamma(\psi(3770) \rightarrow \pi^+ \pi^- J/\psi) = 73 \pm 11$ keV, and $\Gamma(\chi_{c2} \rightarrow \pi^+ \pi^- \eta_c) < 43$ keV. This is generally understood to be a consequence of the OZI rule [125], which (in modern language) says that processes in which the Feynman diagram can be split in two by only cutting internal gluon lines will be suppressed. This is the case for hadronic transitions between charmonium states, as indicated in Fig. 16a.

For standard charmonium states that are above the open-charmed threshold, diagrams for decays to $D^{(*)}\bar{D}^{(*)}$ final states, as shown in Fig. 16b, are not OZI suppressed and partial widths for these “fall-apart” modes are substantially larger. For cases where they have been measured, the OZI suppression factors are more than a hundred [21]:

$$\frac{\Gamma(\psi(3770) \rightarrow D\bar{D})}{\Gamma(\psi(3770) \rightarrow \pi^+ \pi^- J/\psi)} \simeq 350; \quad \frac{\Gamma(\psi(4040) \rightarrow D^{(*)}\bar{D}^{(*)})}{\Gamma(\psi(4040) \rightarrow \eta J/\psi)} \simeq 150. \quad (6.1)$$

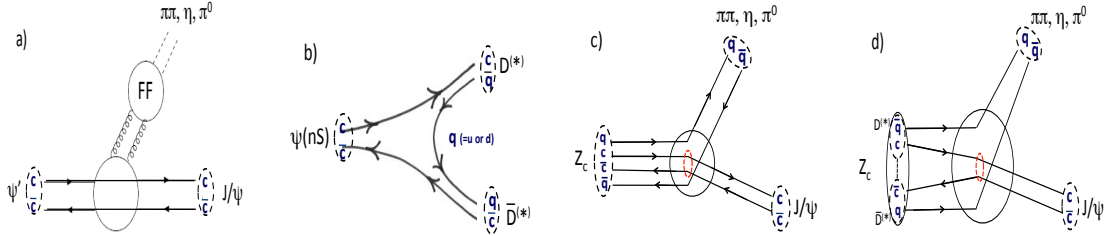


Figure 16: **a)** A diagram for $\psi' \rightarrow \pi^+ \pi^- J/\psi$. Since no quark lines connect the light hadron system to the initial state, this process is expected to be OZI suppressed. **b)** The OZI-allowed “fall-apart” decays to open-charmed-meson pairs that are dominant for $c\bar{c}$ states with masses that are above open-charmed threshold. **c)** OZI-allowed decays of a QCD-tetraquark to light hadrons plus a J/ψ . **d)** A cartoon of a $D^{(*)}\bar{D}^{(*)}$ “molecule” decaying to light hadrons plus a J/ψ .

Since the Z_c states are electrically charged, their minimal structure must be $cq_i\bar{c}\bar{q}_j$, $q_{1(2)} = u(d)$, and OZI suppression is easily evaded. Figure 16c shows a sketch of how a QCD tetraquark could decay via an OZI-allowed hadronic transition to a J/ψ . In a pure molecular picture, one would expect the same transition to be suppressed relative to $D^{(*)}\bar{D}^{(*)}$ fall-apart decays even though the OZI rule is not violated. As illustrated in Fig. 16d, a molecular configuration is an extended object in which the c - and \bar{c} -quarks exist in distinct, color-singlet $D^{(*)}$ and $\bar{D}^{(*)}$ mesons, each with a spatial extent of order 1 fm. These $D^{(*)}$ and $\bar{D}^{(*)}$ mesons are expected to be separated by a similar distance. Since they reside in distinct color-singlet systems, the colors of the c - and \bar{c} -quarks are uncorrelated. In order to form a J/ψ , the c and \bar{c} colors must match *and* they should have considerable overlap in a spatial region with volume of order $\langle r_{J/\psi} \rangle^3$, where $\langle r_{J/\psi} \rangle \simeq 0.4$ fm is the mean c - \bar{c} separation in the J/ψ [107]. This is in contrast to a QCD tetraquark, in which the c and \bar{c} start out being both color correlated and in close proximity.

The partial widths for $Z_c(3900) \rightarrow \pi J/\psi$ and $Z_c(4020) \rightarrow \pi h_c$ are smaller than those for $D\bar{D}^*$ and $D^*\bar{D}^{(*)}$, respectively, but not by very large factors [70, 72]:

$$\frac{\Gamma(Z_c(3900) \rightarrow D\bar{D}^*)}{\Gamma(Z_c(3900) \rightarrow \pi J/\psi)} = 6.2 \pm 3.0; \quad \frac{\Gamma(Z_c(4020) \rightarrow D^*\bar{D}^*)}{\Gamma(Z_c(4020) \rightarrow \pi h_c)} = 12 \pm 5. \quad (6.2)$$

Although no data exist for either $Z_c(4200)$ or $Z(4430)$ decays to $D^{(*)}\bar{D}^{(*)}$ final states, if one assumes that the branching fractions for $B \rightarrow KZ_c(4200)$ and $B \rightarrow KZ(4430)$ are no larger than the PDG upper limit for $\mathcal{B}(B^+ \rightarrow K^+ X(3872)) < 3.2 \times 10^{-4}$, existing data [76, 79] can be used to infer branching fraction *lower* limits of $\mathcal{B}(Z_c(4200) \rightarrow \pi J/\psi) > 4\%$ and $\mathcal{B}(Z(4430) \rightarrow \pi \psi') > 7\%$, which imply large partial widths of order 10 MeV or larger for hadronic transitions to standard charmonium states.¹⁰ This suggests that these states are not pure $D^{(*)}\bar{D}^{(*)}$ molecules but, instead, are hybrid-like structures that contain a tightly bound diquark-diantiquark core. The mass spectrum of these states would then reflect the underlying diquark-diantiquark dynamics, modified by the influence of nearby $D^{(*)}\bar{D}^{(*)}$ thresholds.

6.2 The observed spectrum of $J^P = 1^+$ states

Figure 17 shows the spectrum of $J^P = 1^+$ states discussed in the previous two sections, along with their dominant decay modes. The horizontal dashed lines indicate the $m_D + m_{D^*}$, $2m_{D^*}$, and $m_D + m_{D^*(2S)}$ open-charmed thresholds. All of the states lie near an open-charmed threshold with the notable exception of the recently discovered $Z(4200)$. In accord with the hybrid model for the $X(3872)$ discussed above in Section 4.4.3 and in the spirit of Gell-Mann’s Totalitarian Principle for Quantum Mechanics: “*Everything not forbidden is compulsory* [127],” I attach cartoons next to each state suggesting a QCD core component that mixes with open charmed meson-antimeson pairs ($D^{(*)}\bar{D}^{(*)}$) if their threshold is nearby in mass. For the $X(3872)$, the simplest assumption for the core component is the χ'_{c1} , although this could probably coexist with some admixture of $cu\bar{c}\bar{u}$ and $cd\bar{c}\bar{d}$ tetraquarks. For the various isovector Z states, the simplest core states would be $cq_i\bar{c}\bar{q}_j$, where $q_{1(2)} = u(d)$.

¹⁰The lowest-order diagram for $B \rightarrow KX(3872)$ is “factorizable.” In contrast, the lowest-order $B \rightarrow KZ_c(4200)$ and $B \rightarrow KZ(4430)$ decay processes are non-factorizable. Non-factorizable processes are expected to be suppressed relative to factorizable ones. For a discussion about factorization in B -meson decays, see Ref. [126].

Since the tetraquark core components are not bound by the OZI rule, and have color-correlated c - and \bar{c} -quarks in close proximity, these could account for the large hidden-charm decay partial widths that are seen for the Z states. The effect of coupled-channel $D^{(*)}\bar{D}^{(*)}$ pairs might be forcing some of the Z states toward the open-charmed thresholds, similar to the way the $c\bar{c}$ - $D\bar{D}^*$ couplings lower the mass of the $c\bar{c}$ core in the hybrid model for the $X(3872)$ [103]. Also, if, somehow, the $c\bar{c}$ pairs in the core states are somehow mostly configured in triplet $1S$, singlet $1P$, and triplet $2S$ configurations for the $Z_c(3900)$, $Z_c(4020)$ and $Z_c(4430)$, respectively, that could cause the peculiar pattern where $\pi J/\psi$, πh_c and $\pi\psi'$ decays dominate for the three different states. (Note that the $Z(4430)$ - $Z_c(3900)$ mass splitting (587 ± 20 MeV) is close to $m_{\psi'} - m_{J/\psi} = 589$ MeV.)

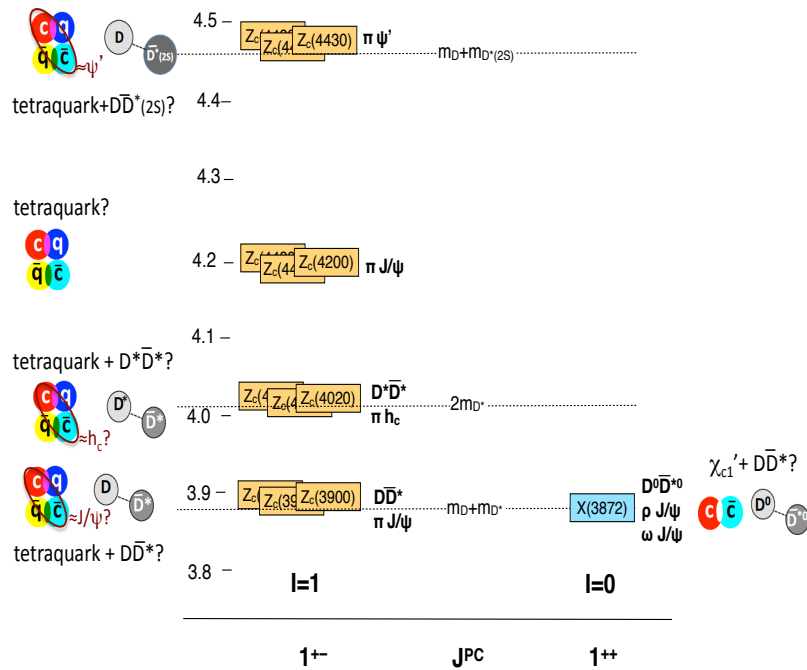


Figure 17: A summary of the $J^P = 1^+$ X and Z charmoniumlike mesons that have been seen to date. All of them are near open-charmed meson thresholds with the notable exception of the recently discovered $Z_c(4200)$. Possible core and meson components are indicated. Here the C -parity assignment of the isovector states refers to that of the neutral member.

6.3 Additional states?

The spectrum depicted in Fig. 17 suggests the possibility of other related states, some of which are indicated in Fig. 18. These are labeled Z_c (“3872”), the mostly isovector partner of the $X(3872)$ discussed above in Section 4.4.3, X_c (“3900”), an isoscalar 1^{+-} partner of the $Z_c(3900)$, and X_2 (“4020”) a version of the $X(3872)$ located at the $D^*\bar{D}^*$ threshold. Here I briefly discuss each of these.

The Z_c (“3872”) As discussed above, this might be a mostly isovector hybrid state with a large D^+D^{*-} component. The $\rho J/\psi$ decay mode would be isospin favored and, if it were significant, this state would probably have been already found. However, if the Z_c (“3872”) mass is near or above $m_{D^+} + m_{D^{*-}} = 3879.9$ MeV, decays to $D\bar{D}^*$ final states might be strong, resulting in a wide natural width and a small branching fraction for $\rho J/\psi$. The $Z_1(4050) \rightarrow \pi\chi_{c1}$ peak reported by Belle [74] could have the correct J^{PC} quantum numbers (to date, nothing is known about its J^P values), but its mass seems too high.

The X_c (“3900”) If this state exists and, in analogy to the $X(3872)$, has a hybrid $c\bar{c}-D\bar{D}^*$ structure, the $h_c(2P)$ (h'_c) would have the right mass and quantum numbers to be its $c\bar{c}$ core state. No evidence is seen for a structure in the $M(\eta J/\psi)$ distribution for $B \rightarrow K\eta J/\psi$ decays [128]. However, 1^{+-} quantum numbers do not seem to be strongly produced in this B decay process; $h_c(1P)$ production has not been seen in B meson decays and a 90% CL upper limit of $\mathcal{B}(B^+ \rightarrow K^+ h_c) < 0.037 \times \mathcal{B}(B^+ \rightarrow K^+ J/\psi)$ has been established [21]. One strategy might be to look for $e^+e^- \rightarrow \pi^+\pi^- X_c$ (“3900”); X_c (“3900”) $\rightarrow \eta J/\psi$ or $D\bar{D}^*$ in the $\sqrt{s} = 4.36$ GeV BESIII data. This would be far enough above threshold for a $\pi^+\pi^- X_c$ (“3900”) to be detectable and a substantial, ~ 50 pb cross section for the related $e^+e^- \rightarrow \pi^+\pi^- h_c$ process has been reported at this energy [71].

The X_2 (“4020”) There are no reports of a structure in the $\pi^+\pi^- J/\psi$ invariant mass distribution in the vicinity of the $D^*\bar{D}^*$ mass threshold even though many experiments have studied this system. However, the Q value for transitions between a state with mass near $2m_{D^*}$ and the J/ψ would be $\simeq 920$ MeV, well above the mass of the ω and, therefore, the isospin-conserving $\omega J/\psi$ transition would likely be dominant. The $\omega J/\psi$ invariant mass distribution has not been well studied. The BaBar experiment studied $\omega J/\psi$ systems produced in $B \rightarrow K\omega J/\psi$ decays using their full, 426 fb^{-1} data sample. They show an intriguingly high data point in the $M(\omega J/\psi)$ distribution near 3990 MeV but with limited statistical significance [42]. The only reported Belle study of the same channel is based on a 253 fb^{-1} data sample, which is only about one third of the full Belle data set. Another promising avenue for this search might be the $D^*\bar{D}^*$ system in $B \rightarrow KD^*\bar{D}^*$ decays. The only reported results for this channel are BaBar measurements of the branching fractions $\mathcal{B}(B \rightarrow KD^*\bar{D}^*)$ [129], which are large: e.g., $\mathcal{B}(B^0 \rightarrow K^+ D^{*-} D^{*0}) = (1.06 \pm 0.03 \pm 0.09)\%$.

7. Summary

I think that now it is safe to conclude that four-quark states have been observed. In fact, there are a sufficient number of established $J^P = 1^+$ four-quark candidate states to reconstruct at least a partial mass spectrum. The initially proposed purely molecule-like and purely diquark-diantiquark explanations for these states cannot reproduce their measured properties. Some of the observed states are near meson-antimeson thresholds, and have many properties that are similar to those expected for kinematically induced threshold cusps. However, these explanations fail to stand up well under close scrutiny.

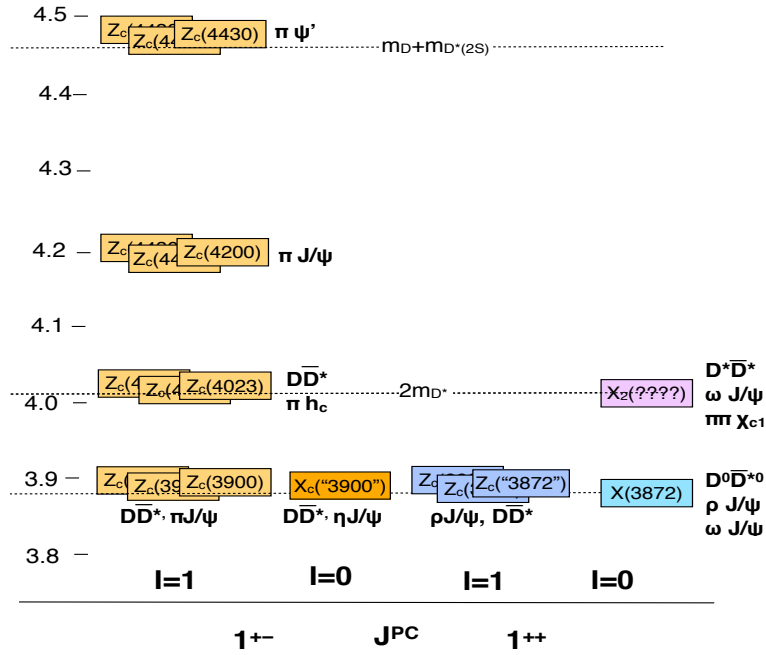


Figure 18: Possibly additional low-lying XYZ states discussed in the text are indicated. Here $Z_c(“3872”)$ indicates the possible 1^{++} , mostly isovector partner of the $X(3872)$ discussed in Section 4.4.3, the $X_c(“3900”)$ would be a 1^{--} mostly isoscalar partner of the $Z_c(3900)$ and the $X_2(“4020”)$ would be a counterpart of the $X(3872)$ near the $D^* \bar{D}^*$ threshold.

The data seem to be telling us that rather than simple molecules of diquark-antidiquark substructures, the observed states are hybrid configurations that consist of molecule-like meson-antimeson pairs coupled to a tightly bound quark-antiquark or diquark-antidiquark core.

This remains a data driven field where significant progress depends mainly on experimental observations of additional states and better measurements of the properties of existing states. To date, most initial observations have involved final states containing a J/ψ or a ψ' (or a narrow Υ state), mostly because these are the simplest channels to access experimentally. However, the BESIII experiment has managed to isolate high-statistics, exclusive h_c signals with rather small backgrounds, and this resulted in the discovery of the $Z_c(4020)$. More comprehensive studies of $D^{(*)} \bar{D}^{(*)}$ final states will be difficult experimentally, but may be well worth the effort.

There is a high interest in this subject and I expect it will continue to be a major emphasis of the BESIII, CMS and LHCb research programs. We can also look forward to future results from BelleII [130] and PANDA [131].

8. Acknowledgements

I congratulate the organizers of Bormio-2015 for arranging another informative and stimulating meeting, and thank them for giving me the opportunity to present this talk. This work was supported by the Institute for Basic Science (Korea) under Project Code IBS-R016-D1.

References

- [1] C.B. Lang, L. Leskovec, D. Mohler and S. Prelovsek arXiv:1503.05363 [hep-lat] and S. Prelovsek and L. Leskovec, Phys. Rev. Lett. **111**, 192001 (2013).
- [2] R.L. Jaffe Phys. Rev. D **17**, 1444 (1978).
- [3] M.B. Voloshin and L.B. Okun, JETP Lett. **23**, 333 (1976); M. Bander, G.L. Shaw and P. Thomas, Phys. Rev. Lett. **36**, 695 (1976); A. De Rujula, H. Georgi and S.L. Glashow, Phys. Rev. Lett. **38**, 317 (1977); A.V. Manohar and M.B. Wise, Nucl. Phys. B **339**, 17 (1993).
- [4] For interesting reviews of this subject and its history, see R.A. Schumacher, arXiv:nucl-ex/051204, and K.H. Hicks, Eur. Phys. J. H **37**, 1 (2012).
- [5] T. Nakano *et al.* (LEPS Collaboration), Phys. Rev. Lett. **91**, 012002 (2003); V.V. Barmin *et al.* (DIANA Collaboration), Phys. Atom. Nucl. **66**, 1715 (2003); S. Stepanyan *et al.* (CLAS Collaboration), Phys. Rev. Lett. **91**, 252001 (2003); J. Barth *et al.* (SAPHIR Collaboration), Phys. Lett. B **572**, 127 (2003); C. Alt *et al.* (NA49 Collaboration), Phys. Rev. Lett. **92**, 042003 (2004).
- [6] See B. McKinnon *et al.* (CLAS Collaboration), Phys. Rev. Lett. **96**, 012002 (2006), K. Shirotori *et al.*, Phys. Rev. Lett. **109**, 132002 (2012) and references cited therein.
- [7] W.-M. Yao, *et al.* (Particle Data Group), J. Phys. G: Nucl. Part. Phys. **33**, 1 (2006), see, in particular, the “Pentaquark Update” by G. Trilling on page 1019.
- [8] Reported by T.E. Barnes in arXiv:hep-ph/0510365.
- [9] R.L. Jaffe, Phys. Rev. Lett. **38**, 1953 (1977); S.R. Beane, *et al.* (NPLQCD Collaboration), Phys. Rev. Lett. **106**, 162001 (2011); T. Inoue, *et al.* (HALQCD Collaboration), Phys. Rev. Lett. **106**, 162002 (2011).
- [10] See B.H. Kim *et al.* (Belle Collaboration), Phys. Rev. Lett. **110**, 222002 (2013), and references cited therein.
- [11] R.L. Jaffe, arXiv:hep-ph/0409065v2.
- [12] The possible existence of nucleon-antinucleon mesons was pointed out in E. Fermi and C.N. Yang, Phys. Rev. **76**, 1739 (1949), six years before the discovery of the antiproton.
- [13] L. Adiels *et al.*, Phys. Lett. B **182**, 405 (1986)
- [14] J.Z. Bai *et al.* (BES Collaboration), Phys. Rev. Lett. **110**, 022001 (2003).
- [15] M. Ablikim *et al.* (BES Collaboration), Eur. Phys. J. **C53**, 15 (2008).
- [16] S.B. Athar *et al.* (CLEO Collaboration), Phys. Rev. D **73**, 032001 (2006).
- [17] X.-W. Kang, J. Haidenbauer and U.-G. Meißner, JHEP **1402**, 113 (2014).
- [18] X.-W. Kang, J. Haidenbauer and U.-G. Meißner, arXiv:1502.0088 [nucl-th].
- [19] B. El-Bennich, M. Lacombe, B. Loiseau, and S. Wycech, Phys. Rev. C **79**, 054001 (2009).
- [20] J.-P. Dedonder, B. Loiseau, B. El-Bennich and S. Wycech, Phys. Rev. C **80**, 045207 (2009).
- [21] K.A. Olive *et al.* (Particle Data Group), Chin. Phys. C **38**, 090001 (2014).
- [22] C. Adolph *et al.* (COMPASS Collaboration), arXiv:1501.05732 [hep-ex].
- [23] Bernard Ketzer, these proceedings.

- [24] A. Szczepaniak, M. Swat, A. Dzierba and S. Teige, Phys. Rev. Lett. **91**, 092002 (2003).
- [25] The basic framework used for computing charmonium masses given in S. Godfrey and N. Isgur, Phys. Rev. D **32**, 189 (1985). A recent application of this framework is provided in Ref. [26].
- [26] T. Barnes, S. Godfrey and E.S. Swanson, Phys. Rev. D **72**, 054026 (2005).
- [27] M.H. Seymour, Nucl. Phys. B **436**, 163 (1995).
- [28] A. Esposito, A.L. Guerrieri, F. Piccinini, A. Pilloni and A.D. Polosa, arXiv:1411.5997.
- [29] S.L. Olsen, Front. Phys. **10**, 101401 (2015).
- [30] N. Brambilla *et al.*, Eur. Phys. J. **C71**, 1534 (2011) and
- [31] G.T. Bodwin, E. Braaten, E. Eichten, S.L. Olsen, T.K. Pedlar and J. Russ, arXiv:1307.7425 [hep-ph].
- [32] S.-K. Choi *et al.* (Belle Collaboration), Phys. Rev. Lett. **91**, 262001 (2003).
- [33] S.-K. Choi *et al.* (Belle Collaboration), Phys. Rev. D **84**, 052004 (2011).
- [34] B. Aubert *et al.* (BaBar Collaboration), Phys. Rev. D **71**, 071103 (2005),
- [35] R. Aaij *et al.* (LHCb Collaboration), Phys. Rev. Lett. **110**, 222001 (2013).
- [36] D. Acosta *et al.* (CDF Collaboration), Phys. Rev. Lett. **93**, 072001 (2004),
- [37] D. Acosta *et al.* (CDF Collaboration), Phys. Rev. Lett. **96**, 102002 (2006).
- [38] A. Abulencia *et al.* (CDF Collaboration), Phys. Rev. Lett. **98**, 132002 (2007).
- [39] T. Aaltonen *et al.* (CDF Collaboration), Phys. Rev. Lett. **103**, 152001 (2009),
- [40] V.M. Abazov *et al.* (D0 Collaboration), Phys. Rev. Lett. **93**, 162002 (2004),
- [41] K. Abe *et al.* (Belle Collaboration), arXiv:0505037[hep-ex].
- [42] B. Aubert *et al.* (BaBar Collaboration), Phys. Rev. Lett. **101**, 082001 (2008).
- [43] T. Aushev *et al.* (Belle Collaboration), Phys. Rev. D **81**, 031103 (2010) and G. Gokhroo *et al.* (Belle Collaboration), Phys. Rev. Lett. **97**, 162002 (2006).
- [44] B. Aubert *et al.* (BaBar Collaboration), Phys. Rev. D **77**, 111101 (2010).
- [45] B. Aubert *et al.* (BaBar Collaboration), Phys. Rev. Lett. **102**, 132001 (2009).
- [46] V. Bhardwaj *et al.* (Belle Collaboration), Phys. Rev. Lett. **107**, 132001 (2011).
- [47] R. Aaij *et al.* (LHCb Collaboration), Nucl. Phys. B **886**, 665 (2014).
- [48] R. Aaij *et al.* (LHCb Collaboration), Eur. Phys. Rev. J. C **72**, 1972 (2004),
- [49] S. Chatrchyan *et al.* (CMS Collaboration), **JHEP04**, 154 (2013).
- [50] S.-K. Choi *et al.* (Belle Collaboration), Phys. Rev. Lett. **94**, 182002 (2005).
- [51] S. Uehara *et al.* (Belle Collaboration), Phys. Re Lett. **104**, 092001 (2010).
- [52] J.P. Lees *et al.* (BaBar Collaboration), Phys. Rev. D **86**, 072002 (2012).v.
- [53] P. Pakhlov *et al.* (Belle Collaboration), Phys. Rev. Lett. **100**, 202001 (2008).
- [54] K. Abe *et al.* (Belle Collaboration), Phys. Rev. Lett. **98**, 082001 (2007).
- [55] B. Aubert *et al.* (BaBar Collaboration), Phys. Rev. D **76**, 111105 (2007).

- [56] G. Pakhlova *et al.* (Belle Collaboration), Phys. Rev. D **77**, 011103 (2008).
- [57] C.-Z. Yuan *et al.* (Belle Collaboration), Phys. Rev. Lett. **99**, 182004 (2007).
- [58] T. Aaltonen *et al.* (CDF Collaboration), Phys. Rev. Lett. **102**, 242002 (2009).
- [59] T. Aaltonen *et al.* (CDF Collaboration), arXiv:1101.6058 (unpublished).
- [60] S. Chatrchyan *et al.* (CMS Collaboration), Phys. Lett. **B734**, 261 (2014).
- [61] B. Aubert *et al.* (BaBar Collaboration), Phys. Rev. Lett. **95**, 142001 (2005).
- [62] B. Aubert *et al.* (BaBar Collaboration), arXiv:0808.1543v2 [hep-ex].
- [63] Q. He *et al.* (CLEO Collaboration), Phys. Rev. D **74**, 091104 (2006).
- [64] T.E. Coan *et al.* (CLEO Collaboration), Phys. Rev. Lett. **96**, 162003 (2006).
- [65] B. Aubert *et al.* (BaBar Collaboration), Phys. Rev. Lett. **98**, 212001 (2007).
- [66] X.L. Wang *et al.* (Belle Collaboration), Phys. Rev. Lett. **99**, 142002 (2007).
- [67] G. Pakhlova *et al.* (Belle Collaboration), Phys. Rev. Lett. **101**, 172001 (2008).
- [68] M. Ablikim *et al.* (BESIII Collaboration), Phys. Rev. Lett. **110**, 252001 (2013).
- [69] Z.Q. Liu *et al.* (Belle Collaboration), Phys. Rev. Lett. **110**, 252002 (2013).
- [70] M. Ablikim *et al.* (BESIII Collaboration), Phys. Rev. Lett. **112**, 022001 (2014).
- [71] M. Ablikim *et al.* (BESIII Collaboration), Phys. Rev. Lett. **111**, 242001 (2013).
- [72] M. Ablikim *et al.* (BESIII Collaboration), Phys. Rev. Lett. **112**, 132001 (2014).
- [73] M. Ablikim *et al.* (BESIII Collaboration), Phys. Rev. Lett. **113**, 212002 (2014).
- [74] R. Mizuk *et al.* (Belle Collaboration), Phys. Rev. D **78**, 072004 (2008).
- [75] J.P. Lees *et al.* (BaBar Collaboration), Phys. Rev. D **85**, 052003 (2011).
- [76] K. Chilikin *et al.* (Belle Collaboration), Phys. Rev. D **90**, 112009 (2014).
- [77] S.-K. Choi *et al.* (Belle Collaboration), Phys. Rev. Lett. **100**, 142001 (2008).
- [78] R. Mizuk *et al.* (Belle Collaboration), Phys. Rev. D **80**, 031104(R) (2009).
- [79] K. Chilikin *et al.* (Belle Collaboration), Phys. Rev. D **88**, 074026 (2013).
- [80] R. Aaij *et al.* (LHCb Collaboration), Phys. Rev. Lett. **112**, 222002 (2014).
- [81] K.-F. Chen *et al.* (Belle Collaboration), Phys. Rev. Lett. **100**, 121601 (2008).
- [82] A. Bondar *et al.* (Belle Collaboration), Phys. Rev. Lett. **108**, 122001 (2012).
- [83] A. Garmash *et al.* (Belle Collaboration), arXiv:1403.0092, to appear in Physical Review D. See also:
A. Adachi *et al.* (Belle Collaboration), arXiv:1105.4583.
- [84] I. Adachi *et al.* (Belle Collaboration), arXiv:1209.6450.
- [85] P. Krokovny *et al.* (Belle Collaboration), Phys. Rev. D **88**, 052016 (2013).
- [86] K. Abe *et al.* (Belle Collaboration), Phys. Rev. D **70**, 071102 (2004).
- [87] B. Aubert *et al.* (BaBar Collaboration), Phys. Rev. D **72**, 031101(R) (2005).
- [88] B.Q. Li and K.T. Chao, Phys. Rev. D **79**, 094004 (2009).

- [89] M. Ablikim *et al.* (BESII Collaboration), Phys. Lett. B **660**, 315 (2008).
- [90] Wolfgang Gradl, these proceedings.
- [91] Sören Lange, these proceedings.
- [92] F.-K. Guo and U.-G. Meissner, Phys. Rev. D **86**, 091501 (2012).
- [93] S.L. Olsen, Phys. Rev. D **91**, 057501 (2015).
- [94] M. Ablikim *et al.* (BESIII Collaboration), Phys. Rev. Lett. **112**, 092001 (2014).
- [95] A. Tomaradze, S. Dobbs, T. Xiao and K.K. Seth, Phys. Rev. D **91**, 011102(R) (2015).
- [96] (CDFII Collaboration), CDF note 7159, <http://www-cdf.fnal.gov>.
- [97] E.J. Eichten, K. Lane and C. Quigg, Phys. Rev. D **69**, 094019 (2004) and Phys. Rev. D **73**, 014014 (2006).
- [98] H. Wang, Y. Yang and J. Ping, Eur. Phys. J. A **50**, 76 (2014).
- [99] See, for example, F.E. Close and P.R. Page, Phys. Lett. B **578**, 119 (2003); C.-Y. Wong, Phys. Rev. C **69**, 055202 (2004); S. Pakvasa and M. Suzuki, Phys. Lett. B **579**, 67 (2004); E. Braaten and M. Kusunoki, Phys. Rev. D **69**, 114012 (2004); E.S. Swanson, Phys. Lett. B **588**, 189 (2004); M.B. Voloshin, Phys. Lett. **B604**, 69 (2004); S. Fleming, M. Kusunoki, T. Mehan and U. van Kolck, Phys. Rev. D **76**, 034006 (2007); E. Braaten and M. Lu, Phys. Rev. D **76**, 094028 (2007) & Phys. Rev. D **77**, 014029 (2008); S.L. Zhu, Int. J. Mod. Phys. **E17**, 283 (2009); D. Gamermann and E. Oset, Phys. Rev. D **80**, 014003 (2009); D. Gamermann, J. Nieves, E. Oset and E. Ruiz Arriola, Phys. Rev. D **81**, 014029 (2010); P. Wang and X.G. Wang, Phys. Rev. Lett **111**, 042002 (2013).
- [100] L. Maiani, F. Piccinini, A.D. Polosa and V. Riguer, Phys. Rev. D **71**, 014028 (2005).
- [101] R.D. Matheus, S. Narison, M. Nielsen, and J.-M. Richard, Phys. Rev. D **75**, 014005 (2007); M. Karliner and H.J. Lipkin, arXiv:hep-ph/0601193.
- [102] Yu.S. Kalashnikova, Phys. Rev. D **72**, 034010 (2005); M. Suzuki, Phys. Rev. D **72**, 114013 (2005); O. Zhang, C. Meng and H.Q. Zheng, Phys. Lett. B **680**, 453 (2009); R. D. Matheus, F.S. Navarra, M. Nielsen and C.M. Zanetti, Phys. Rev. D **80**, 056002 (2009); Yu.S. Kalashnikova and A.V. Nefediev, Phys. Rev. D **80**, 074004 (2009); P.G. Ortega, J. Segovia, D.R. Entem and F. Fernandez, Phys. Rev. D **81**, 054023 (2010); I.V. Danilkin and Y.A. Simonov, Phys. Rev. Lett. **105**, 102002 (2010); J. Ferretti, G. Galat'á and E. Santopinto, Phys. Rev. C **88**, 015207 (2013); W. Chen, H.-y. Jin, R.T. Kleiv, T.G. Steele, M. Wang and Q. Xu, Phys. Rev. D **88**, 045027 (2013).
- [103] M. Takizawa and S. Takeuchi, PTEP **2013**, 9, 0903D01 (2013), arXiv:1206.4877 [hep-ph], and S. Takeuchi, K. Shimizu and M. Takizawa, arXiv:1408.0973 [hep-ph].
- [104] S. Coito, G. Rupp and E. van Beveren, Eur. Phys. J. C **71**, 1762 (2011) and Eur. Phys. J. C **73**, 2351 (2013).
- [105] T. Friedmann, Eur. Phys. J. C **73**, 2298 (2013).
- [106] E. Braaten and H.-W. Hammer, Phys. Rept. **428**, 259 (2006).
- [107] J. Eigsperger, arXiv:0707.1269 [hep-ph].
- [108] C. Bignamini, B. Grinstein, F. Piccinini, A.D. Polosa and C. Sabelli, Phys. Rev. Lett. **103**, 162001 (2009) and A.L. Guerrieri, F. Piccinini, A. Pilloni and A.D. Polosa Phys. Rev. D **90**, 034003 (2014).

- [109] E.S. Swanson, Phys. Lett. B **588**, 189 (2004); W. Dong, A. Faessler, T. Gutsche, and V.E. Lyubovitskij, J. Phys. G **38**, 015001 (2011); J. Ferretti and G. Galata, Phys. Rev. D **90**, 054010 (2014).
- [110] L. Maiani, F. Piccinini, A.D. Polosa and V. Riguer, Phys. Rev. D **89**, 114010 (2014).
- [111] B. Aubert *et al.* (BaBar Collaboration), Phys. Rev. D **71**, 031501 (2010).
- [112] L. Maiani, V. Riguer, R. Faccini, F. Piccinini, A. Pilloni and A.D. Polosa, Phys. Rev. D **87**, 111102(R) (2013).
- [113] B. Aubert *et al.* (BaBar Collaboration), Phys. Rev. D **79**, 112001 (2009).
- [114] P. del Amo Sanchez *et al.* (BaBar Collaboration), Phys. Rev. D **82**, 111101(R) (2010).
- [115] C. Zhang, Sci. China G **53**, 2084 (2010).
- [116] M. Ablikim *et al.* (BESIII Collaboration), Nucl. Instrum. Methods A **614**, 345 (2010).
- [117] D.V. Bugg, EPL, **96**, 11002 (2011).
- [118] D.-Y. Chen, X. Liu and T. Matsuki Phys. Rev. D **88**, 036008 (2013).
- [119] E.S. Swanson, arXiv:1409.3291 [hep-ph].
- [120] F.-K. Guo, C. Hanhart, Q. Wang and Q. Zhao, Phys. Rev. D **91**, 051504 (2015).
- [121] E.S. Swanson, arXiv:1504.07952 [hep-ph]
- [122] M. Cleven, F.-K. Guo, C. Hanhart, Q. Wang and Q. Zhao, arXiv:1510.00854 [hep-ph]
- [123] R.G. Ping, private communication.
- [124] C.Z. Yuan, private communication
- [125] S. Okubo, Phys. Lett. **5**, 1975 (1963); G. Zweig, CERN Report No. 8419/TH412 (1964); J. Iizuka, Prog. Theor. Phys. Suppl. **37**, 38 (1966).
- [126] M. Beneke, G. Buchelle, M. Neubert and C. Sachrajda, Nucl. Phys. B **591**, 313 (2000).
- [127] M. Gell-Mann, Il Nuovo Cimento **4** 848 (1956).
- [128] T. Iwashita *et al.* (Belle Collaboration), PTEP **2014**, 043C01 (2014).
- [129] P. del Amo Sanchez *et al.* (BaBar Collaboration), Phys. Rev. D **83**, 032004 (2011).
- [130] T. Abe *et al.* (BelleII Collaboration), arXiv:1011.6352 [hep-ex].
- [131] M.F.M. Lutz *et al.* (PANDA Collaboration), arXiv:0903.3905 [hep-ex].